Ultrafast optical control with single self-assembled quantum dots

M S Skolnick, Department of Physics and Astronomy, University of Sheffield

1. Introduction to quantum dots
2. Spin initialisation, control and readout
3. CROT gate
4. Dressed states
5. Excitation induced dephasing
6. ‘Lamb shift’. Analogy with quantum electrodynamics.
7. Applications of quantum dots
8. Perspectives

The University Of Sheffield.

EPSRC

QIRC

UKIERI
UK-India Education and Research Initiative

Acknowledgements

Experiments: A J Ramsay, S J Boyle, A M Fox, T Godden, A P Heberle

Growth: HY Liu, M Hopkinson

Theory: E M Gauger, A Nazir, B W Lovett (excitation induced dephasing)

Quantum dot lasers: R A Hogg

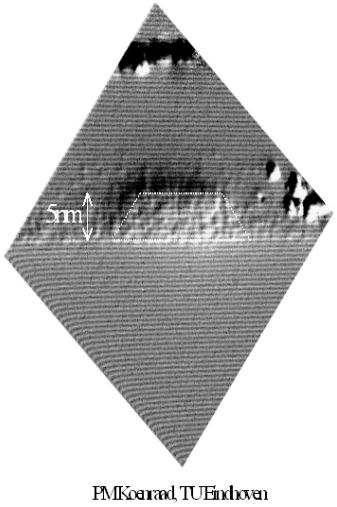

STM

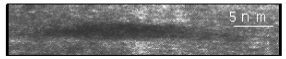

TEM

Growth direction

Self assembled quantum dots: **nanometre scale quantum systems confined strongly in all three dimensions**

Advantages of Self-Assembled Quantum Dots

- Strong confinement and high radiative efficiency
- Two level systems. ‘Atom-like’
- High oscillator strengths, strong interaction with optical fields
- Ultrafast speeds
- Favourable spin properties
- **Focus on In(Ga)As dots in GaAs. Best developed**

Modification of Density of States by Reduction of Dimensionality: underlies all new physics

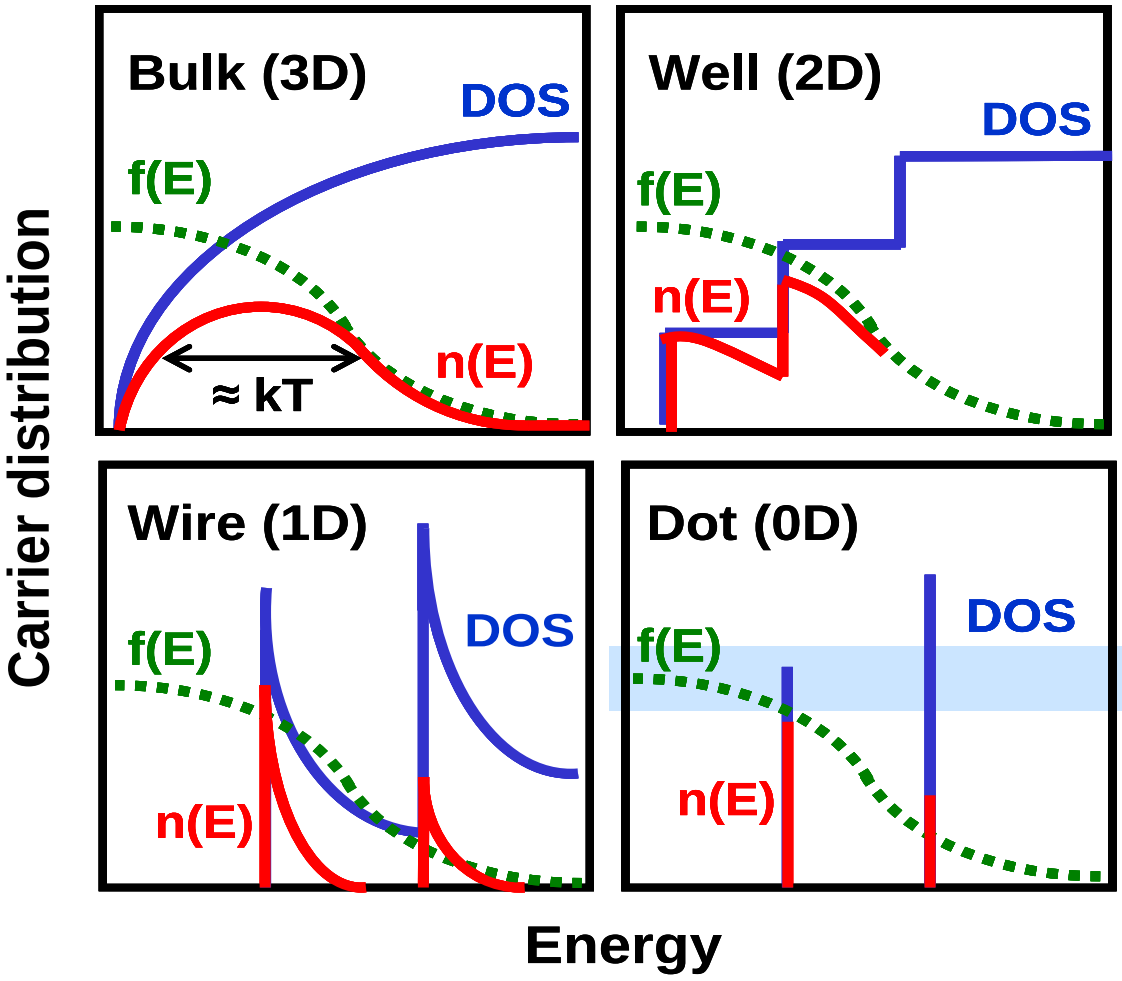

Self-Assembled Crystal Growth in Strained Systems (schematic) MBE Growth

Stranski-Krastanow growth

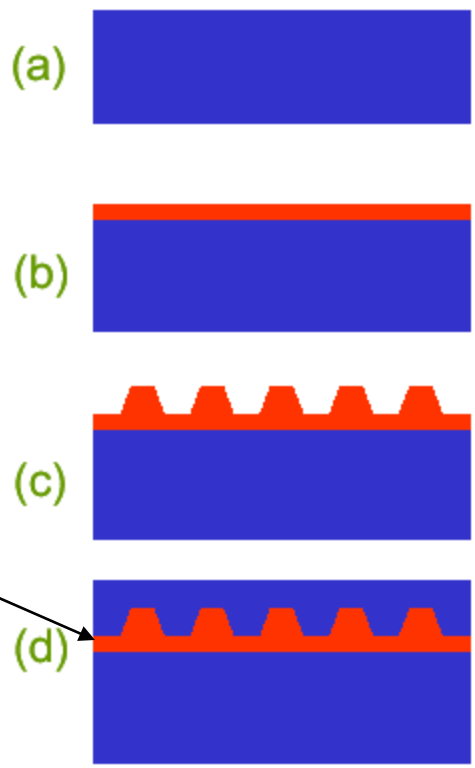

InAs-GaAs 7% lattice mismatch

Note wetting layer

InAs

GaAs

Embedded in crystal matrix – like any other semiconductor laser or light emitting diode

But shape, size, composition fluctuations

Quantum Dots and the Wetting layer

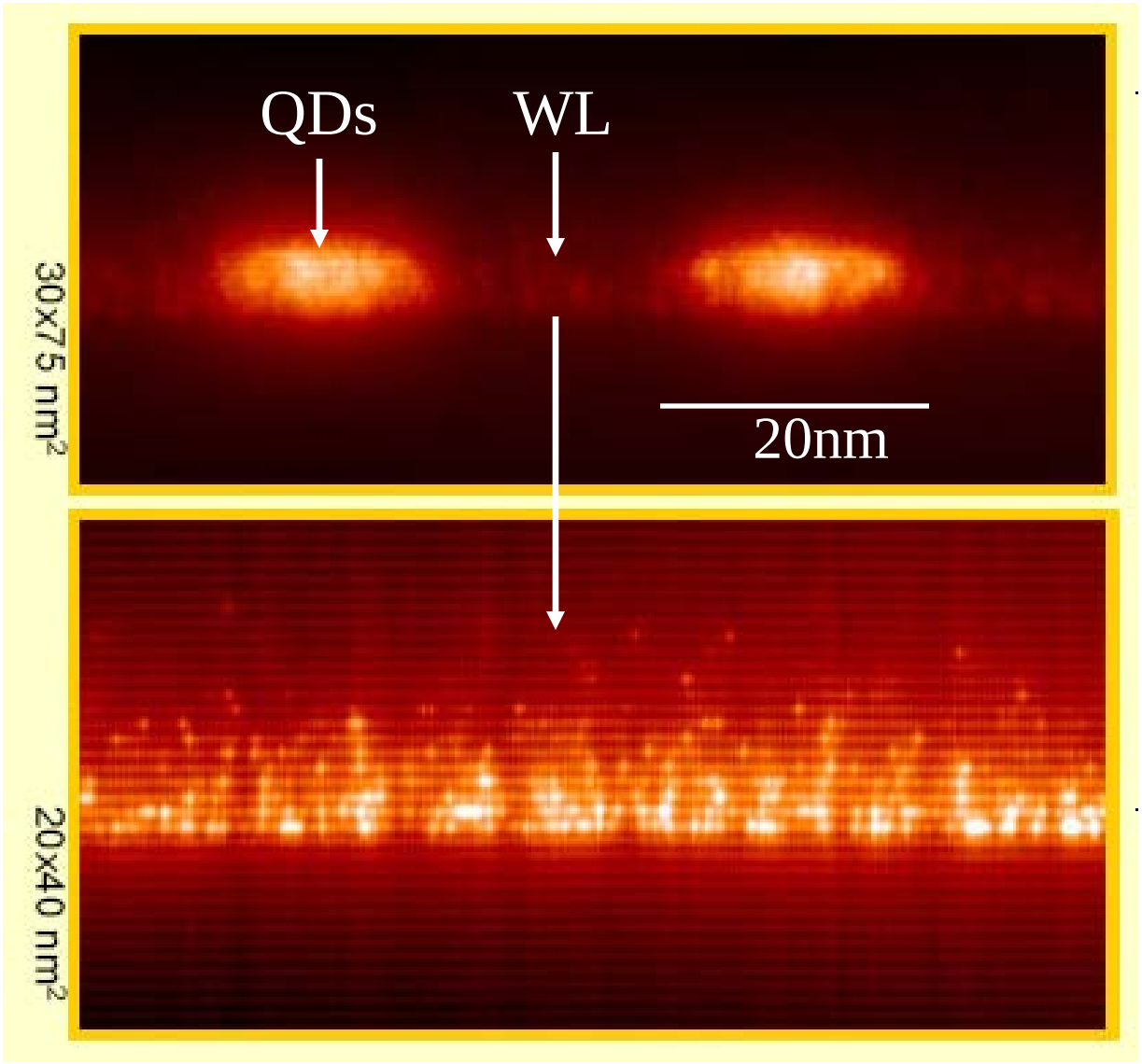

Wetting layer gives rise to continuum which leads to dephasing for excited states

UHV-STM cross sections

PM Koenraad, TU Eindhoven

In(Ga)As Stranski-Krastanow Quantum Dots

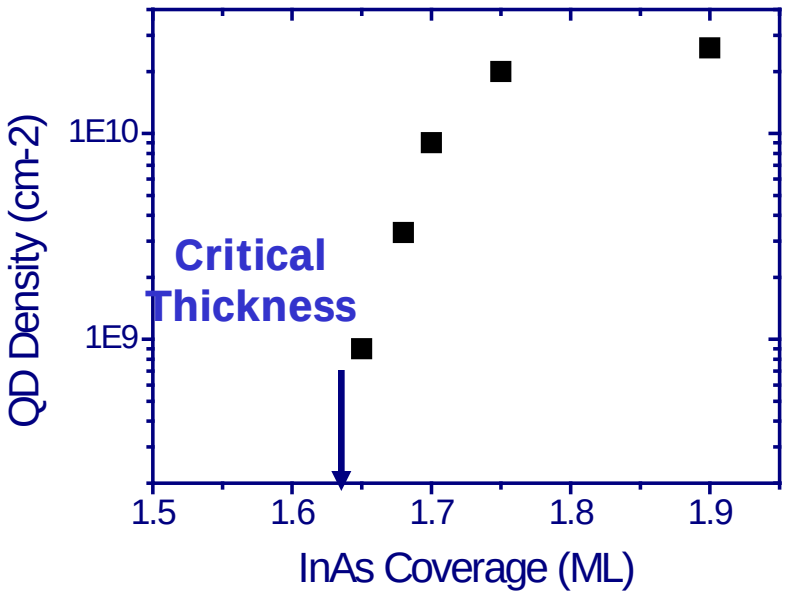

Note density increases rapidly

For this work 1-5x10^{9}cm^{-2}

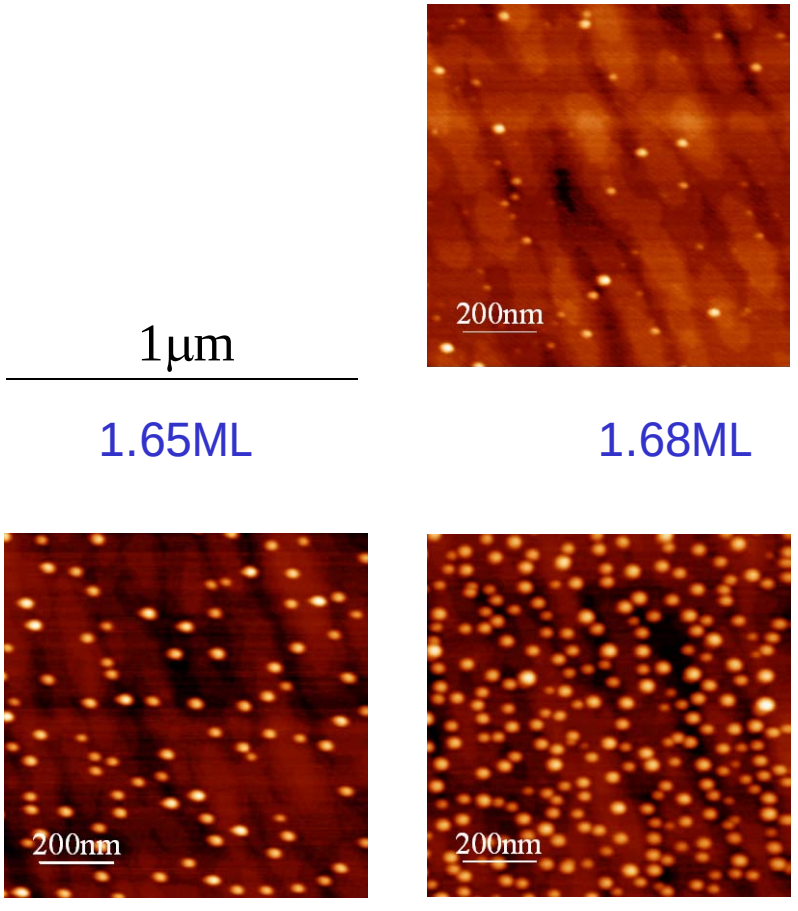

Plan view AFM

Cross section - TEM

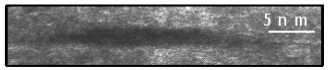

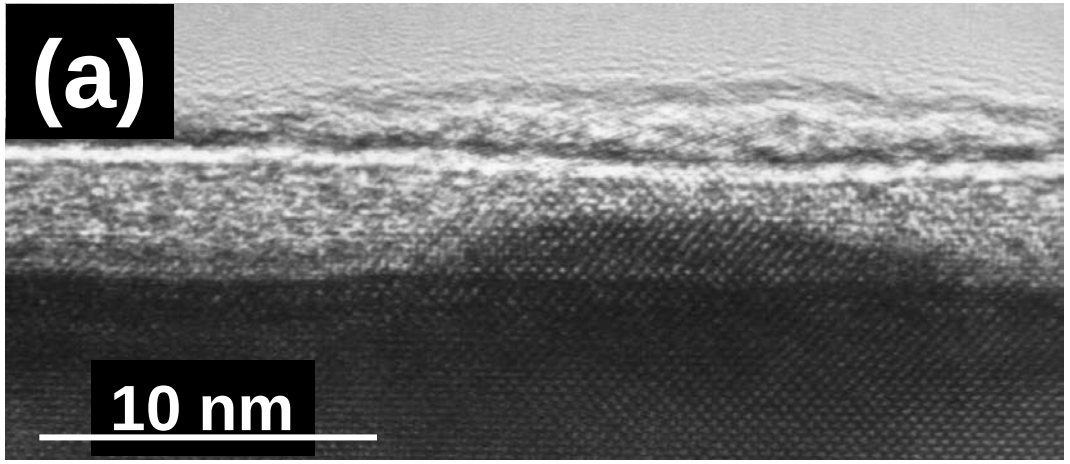

Higher growth rate, 0.3 monolayers/sec, density ~$5x10^{10}cm^{-2}$

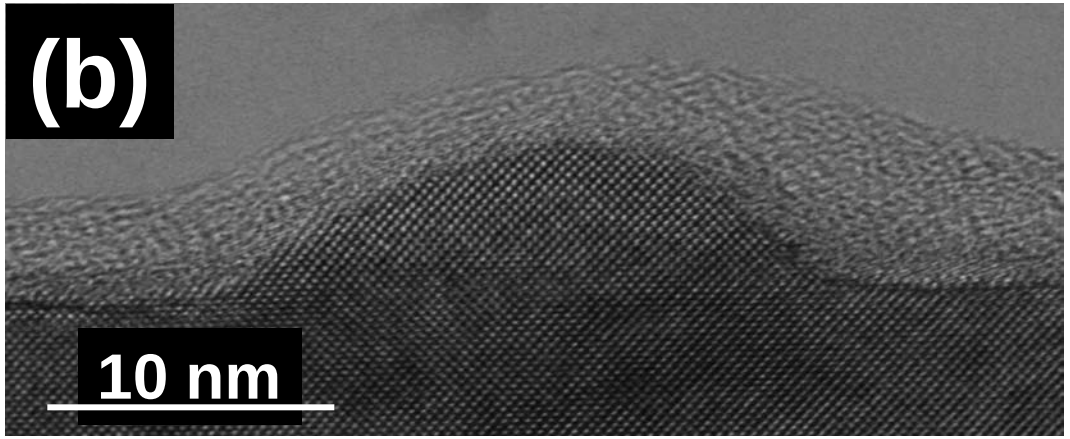

Low growth rate 0.01 monolayers/sec), density ~$3x10^{9}cm^{-2}$

M Hopkinson, AG Cullis, Sheffield

•Energy Level Structure

- Discrete energy levels – atom-like
- Electron energy level splitting 20-70meV, hole levels spaced by ~10meV.
- Favourable for room temperature operation

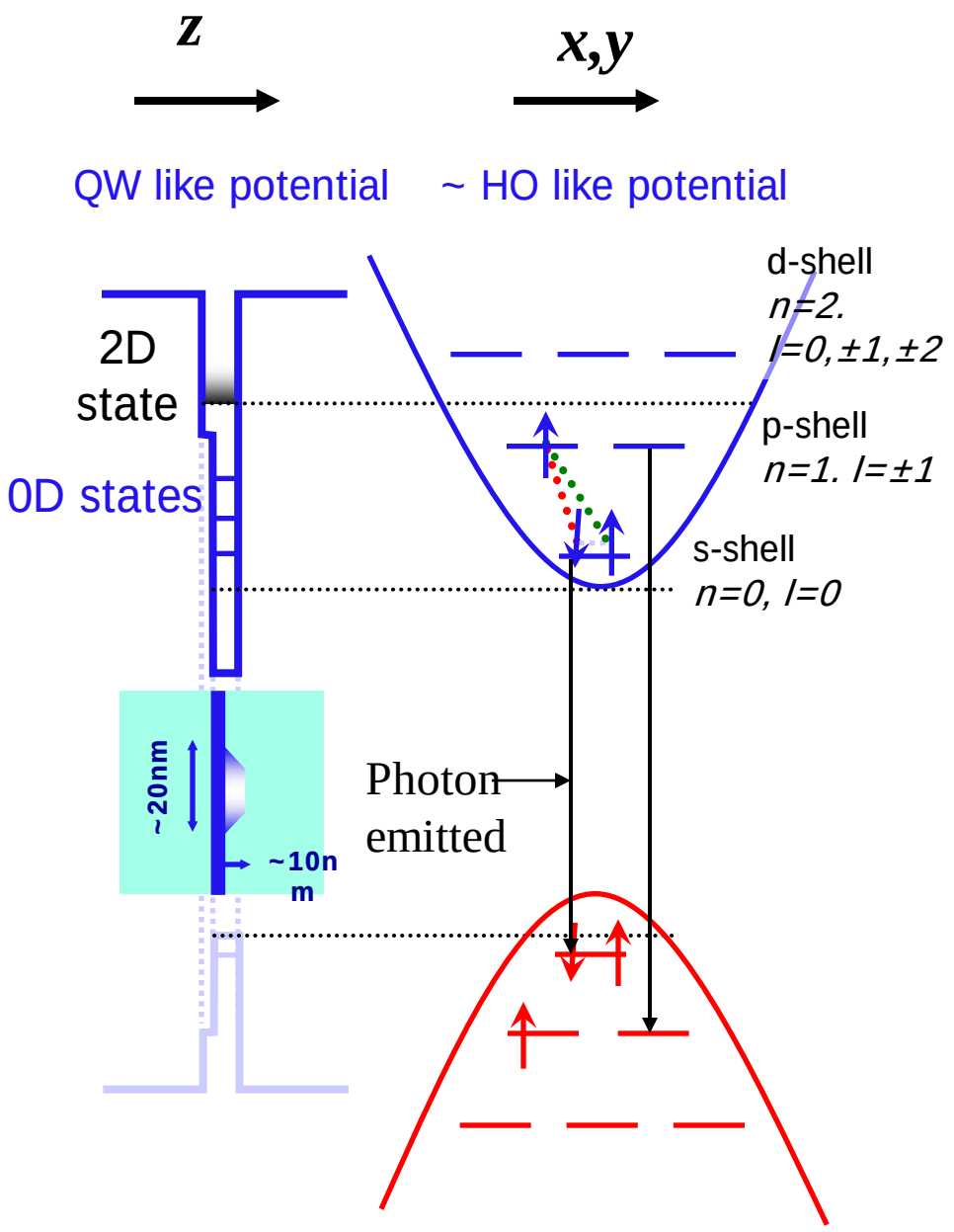

Large Ensembles

- **Introduction to QD electronic structure, composition, shape**

~10^6 – 10^7 dots. Broadening due to shape and size fluctuations

Optical Spectra

emission

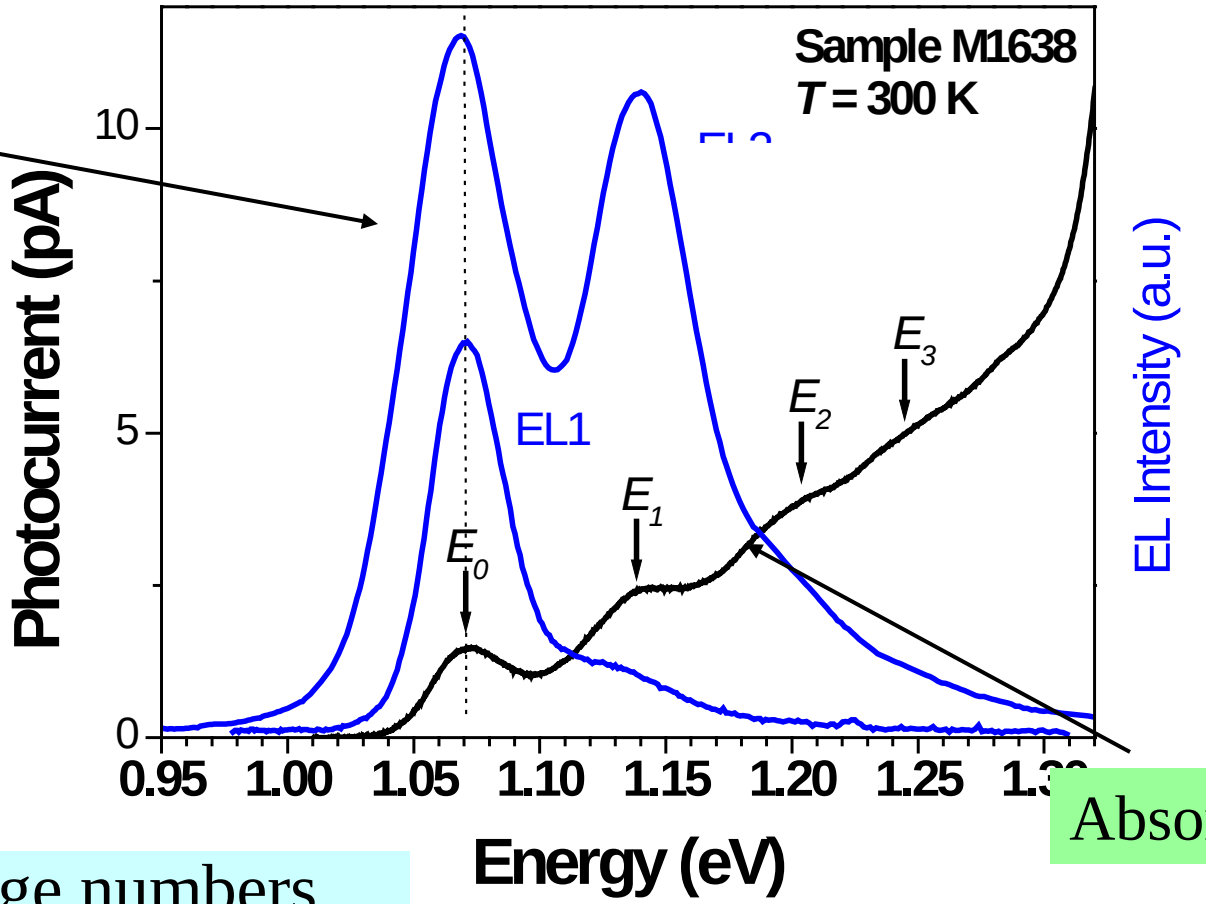

Absorption

Studies of large numbers ~10^7 dots.

Linewidth ~30meV due to shape and size fluctuations

Emission: Spatially resolved PL

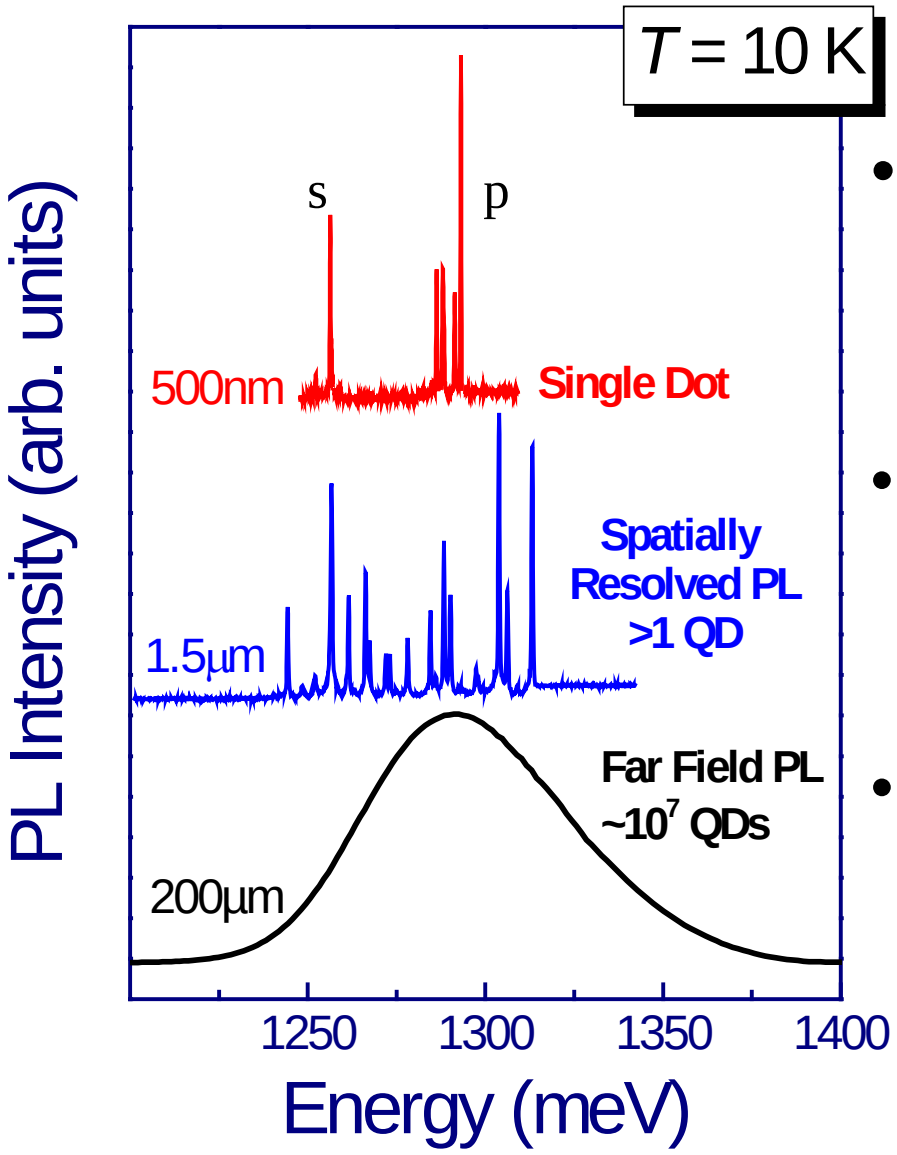

- Single dots may be optically isolated using apertures with ~500nm size.
- Emission spectrum breaks up into sharp lines,
  homogeneous linewidth ~ *1μeV*
- Ground (s-shell) and excited state (p-shell) emission

Evidence for level filling in Quantum Dots, Few Exciton Spectra

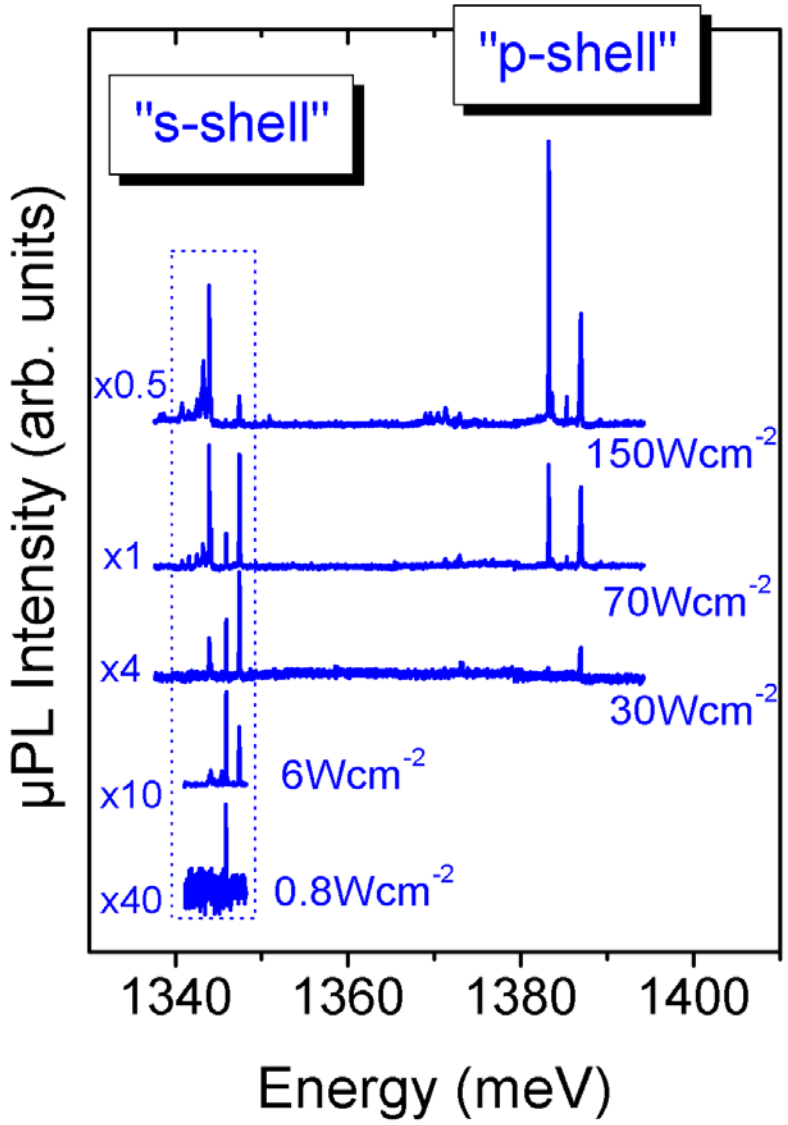

Physical Review B63, 161305R, 2001

- Excitation power density (P_{ex}) controls average exciton occupancy (N_X)

- $N_x << 1$ – single line
- N_X ~ 1-2 – two groups of lines :
  s-shell (~1345meV)
  p-shell (~1380meV)

Evidence for

- Degeneracy of QD levels
- Forbidden transitions

Spins in Quantum Dots

- Quantum dots good approximation to two level systems
- Due to discrete density of states expect scattering to be suppressed relative to higher energy systems
- Electron coherence times (T_2) μsec range
- Ultrafast speeds using optical pulses
- $>10^3$ operations within dephasing times using ~5psec pulses
- InGaAs quantum dots embedded in GaAs matrix

Neutral exciton, X^o

1 electron ($m_e = \pm 1/2$), 1 hole $m_h = \pm 3/2$)

Split by e-h exchange, ~0.3meV

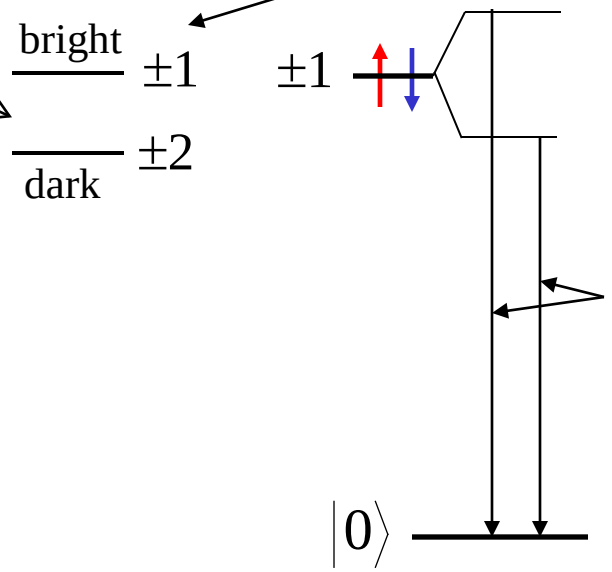

Doublet: linearly polarised (parallel to [110]

Split by anisotropic exchange interaction

$$\mathcal{H}_{exchange} = -\sum_{i=x,y,z} \left(a_i J_{h,i} S_{e,i} + b_i J_{h,i}^3 S_{e,i}\right).$$

S, *J*
e, *h* spins

Charged exciton, X^+

2 holes, 1 electron

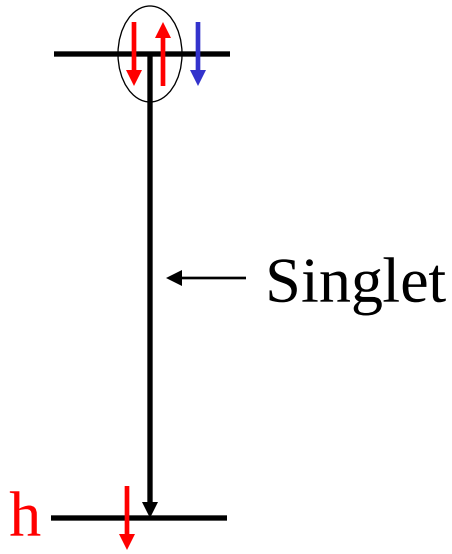

- Charged excitons are important – pure spin eigenstates
- Use trion (charged exciton) transitions to control single carrier spins

2 holes, anti-parallel spin, total spin zero

Exchange interaction quenched

Beats due to fine structure splitting on single dot: pump-probe experiment

T=10K

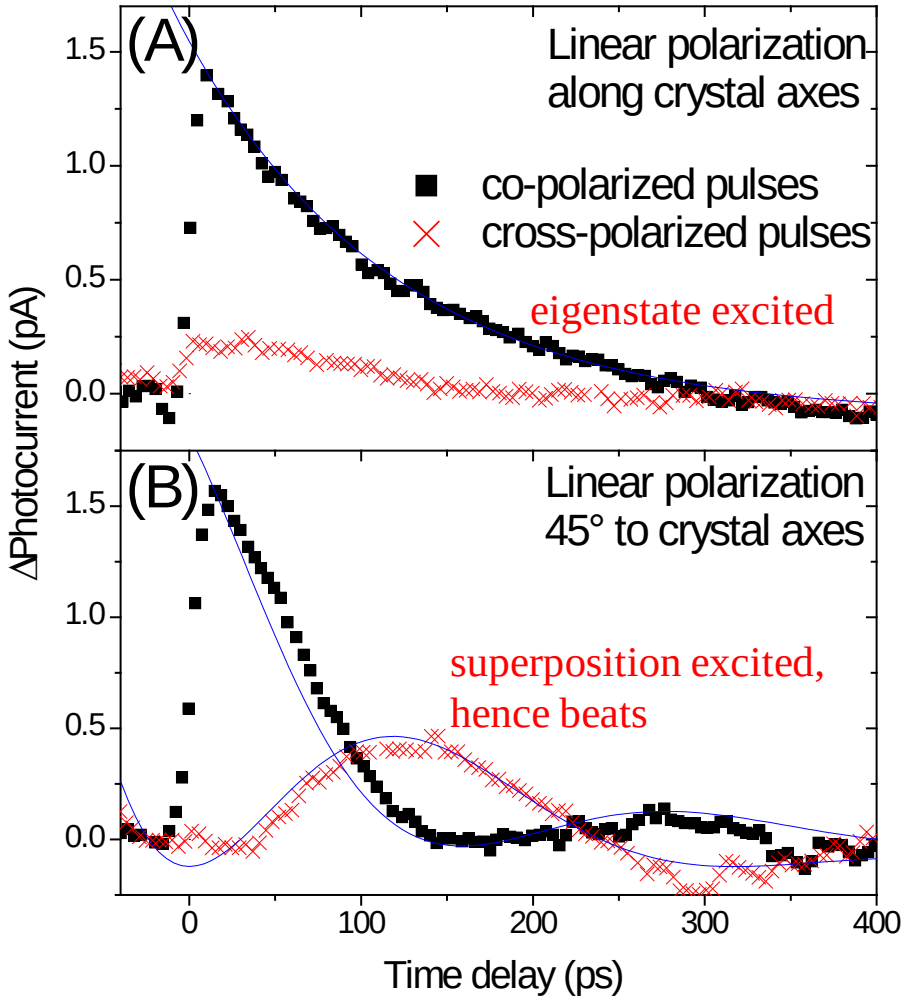

Linearly polarised excitation at 45^{o} to (110) directions (QD axes) : quantum beats since both linearly polarised eigenstates excited

Beats absent for excitation parallel to axes – since only one of eigenstates then excited

Period ~250psec, ~15μeV

Study individual Quantum Dots

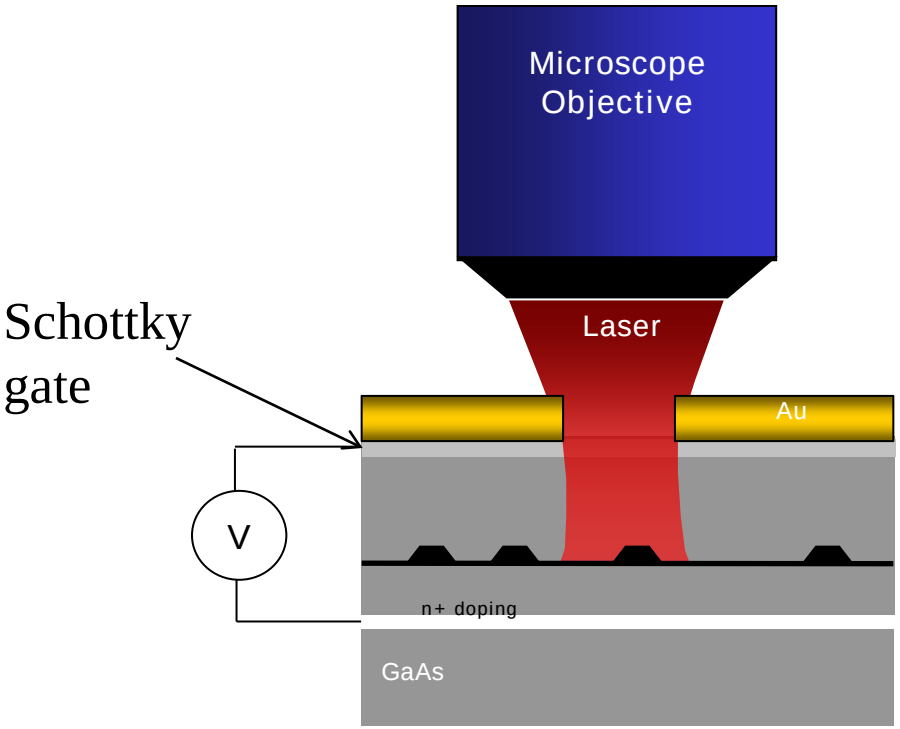

AFM

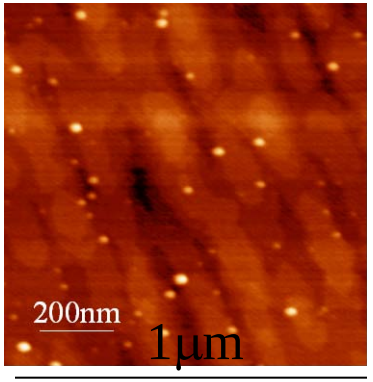

$1\text{-}5\times10^{9}\text{cm}^{-2}$

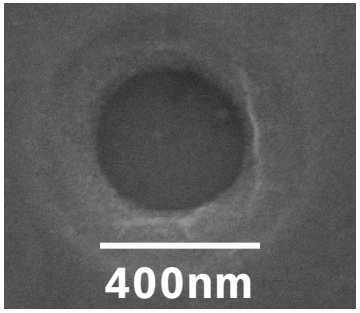

- Principle of **photocurrent measurement**: resonant absorption

- Single QD photodiode

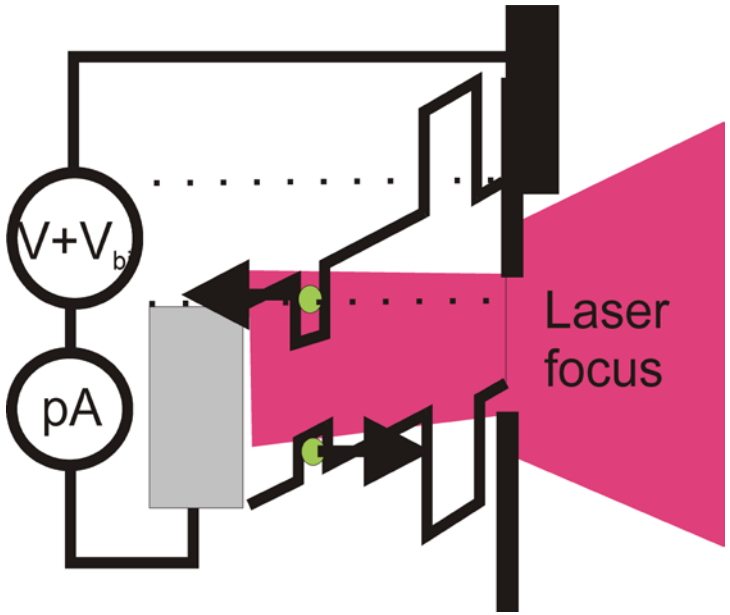

Schematic of photocurrent measurement

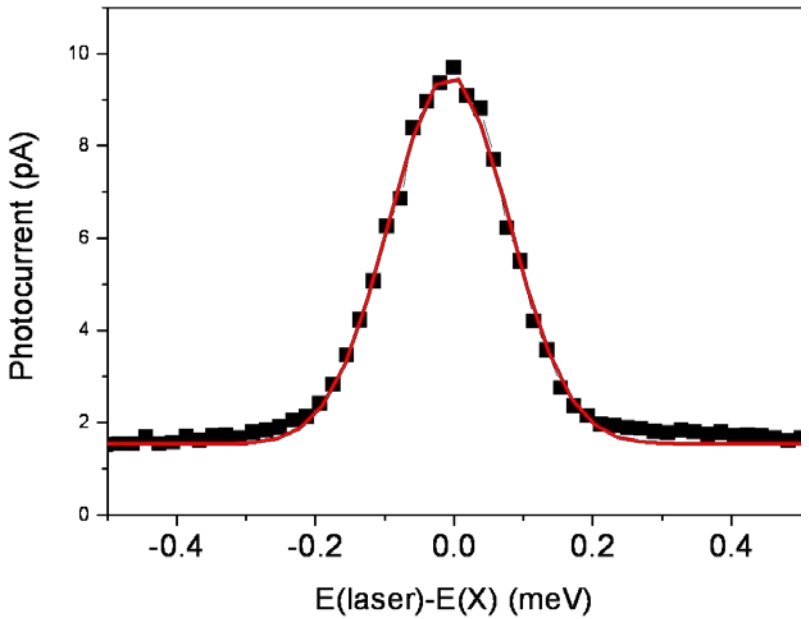

photocurrent spectrum

2 pulse, 2 colour ultrafast system with tunable delay. 10psec pulses (~0.2meV)

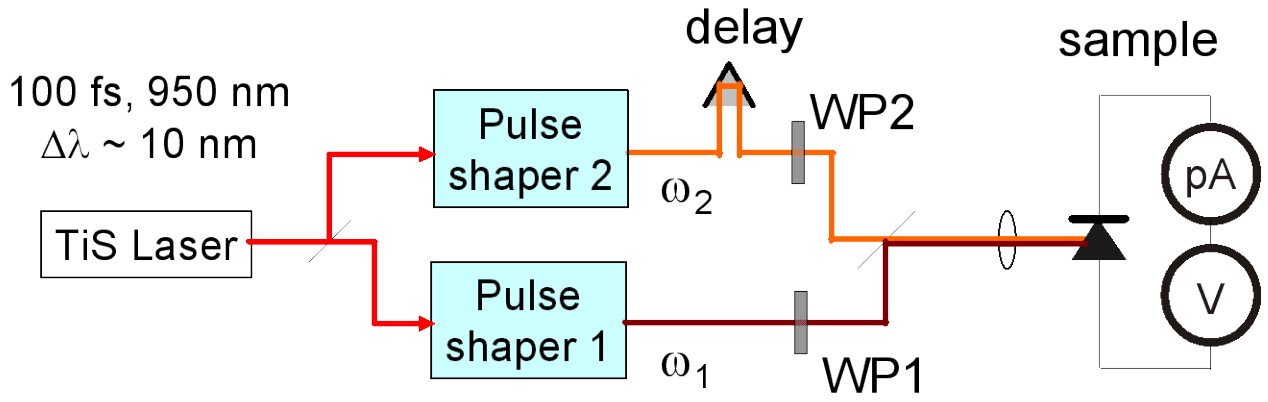

~1 μeV homogeneous linewidths

Photocurrent Detection Techniques

Fundamental to all single dot experiments to be presented

Strong signal on ‘zero’ background

Absorption: very weak signal on large background

1. Ultrafast spin preparation, control and readout of single carrier spins

Use selective tunnelling of one carrier type to prepare spin

Photocurrent detection – quantitative, sensitive readout

Ramsay et al, PRL 100, 187401, 2008

Zrenner et al, Nature 418, 612, 2002 (coherent regime),

Oulton, Finley, PRB 66, 045313, 2002 (photocurrent)

Kroutvar et al Nature 432, 81, 2004 (preparation)

Other related work: Press et al, 2008, Berezovsky et al 2008, Gerardot 2008

Initialisation, control, readout

1: Prepare spin polarized electron-hole pair

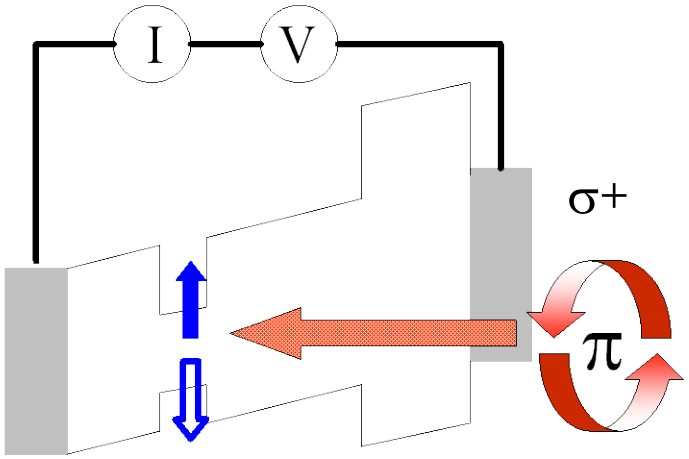

2: Electron tunnels, → spin polarized hole

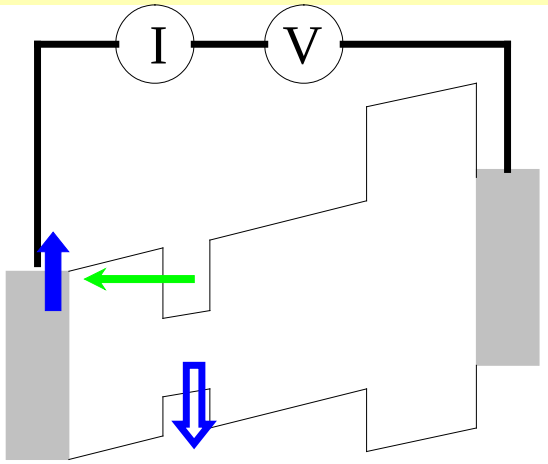

3: Create trion conditional on hole spin, and control phase

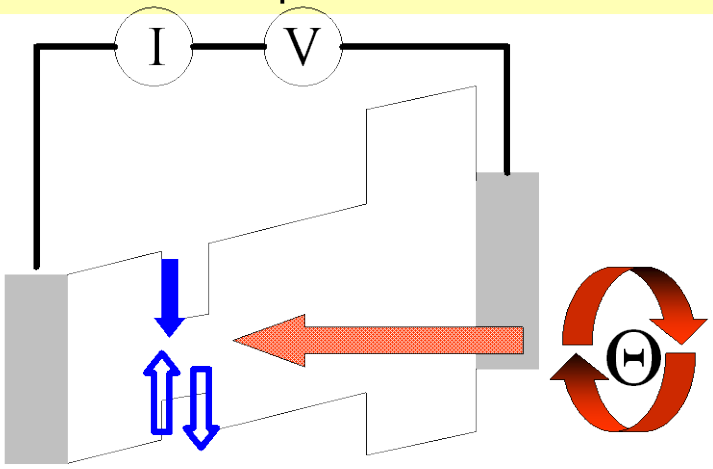

4: Carriers tunnel from dot and are read-out

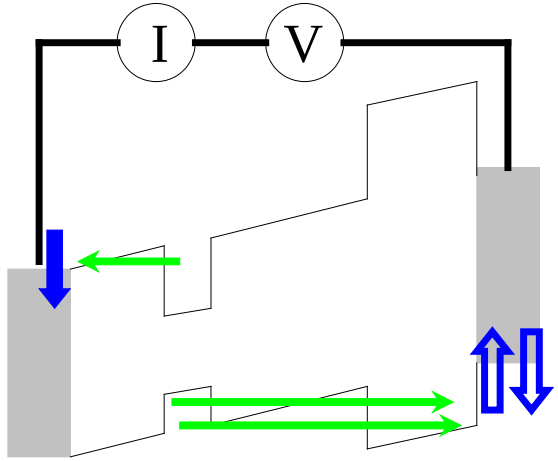

X^0, X^+ spectra in photocurrent

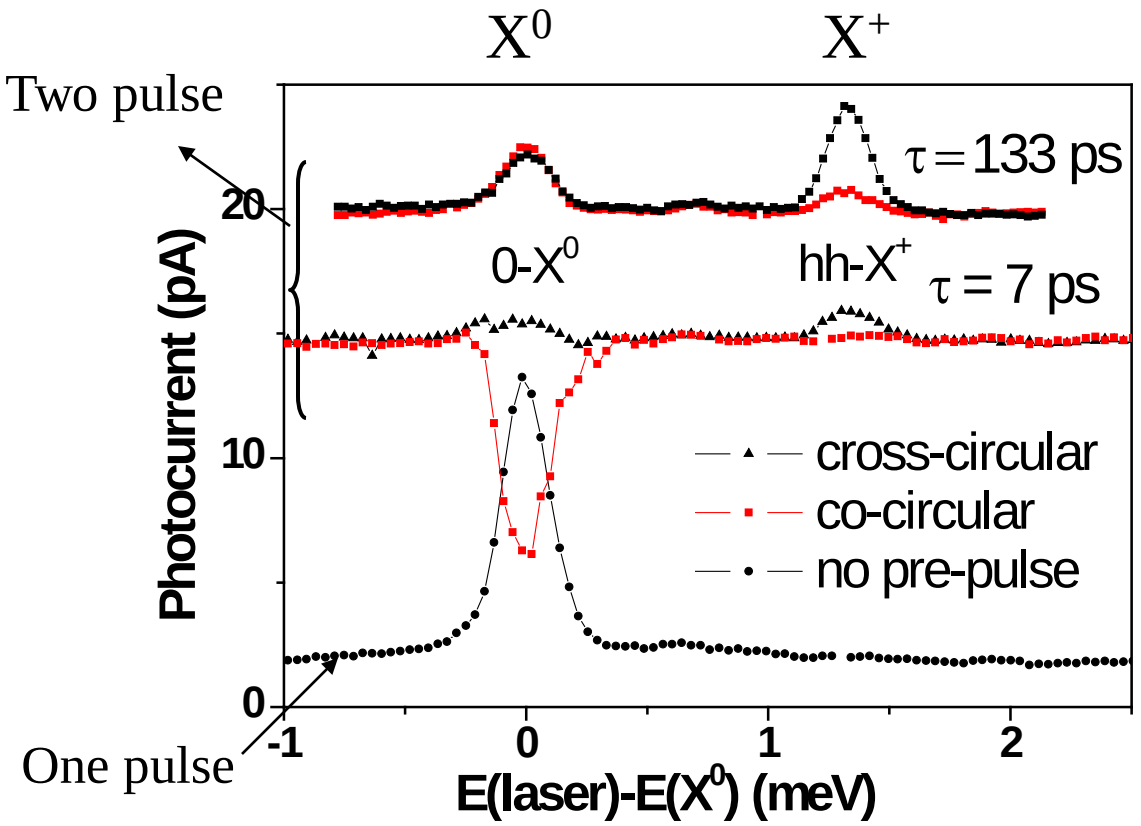

T~10K

π-pulses

X^o behaviour

- First π-pulse creates X^o
- Photocurrent ~11pA
- Close to 12.2pA expected from repitition rate of laser
- Second π-pulse returns system to ground state

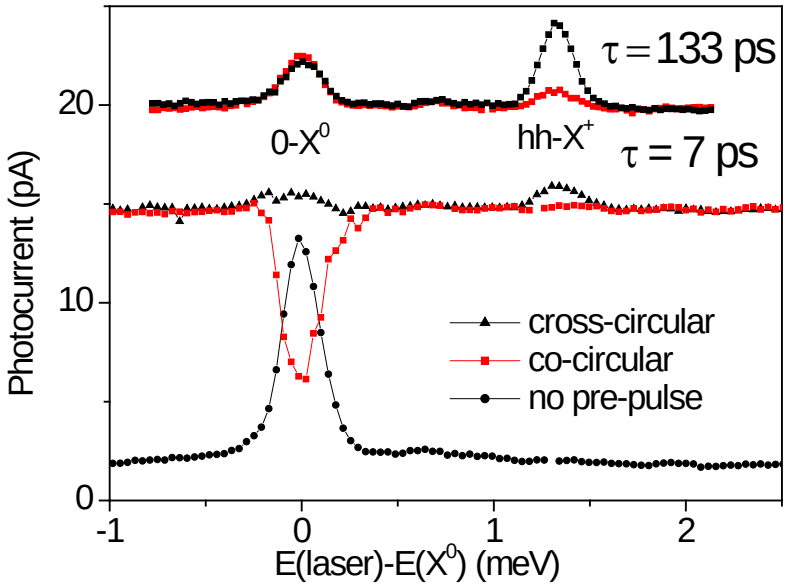

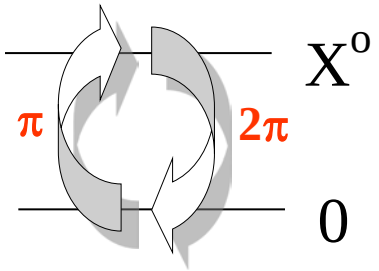

Direct observation in time domain later

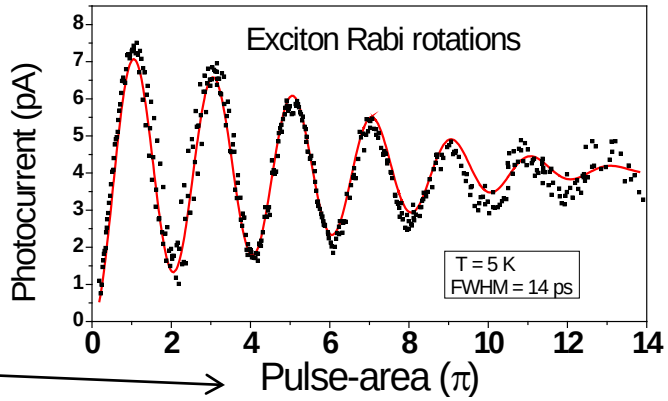

One pulse

$\propto$ (power)$^{1/2}$

Some definitions

Pulse area $\theta(t) = \int \frac{E(t)\mu dt}{\hbar} \propto (\text{power})^{1/2}$

E optical field amplitude, μ dipole moment

Rabi frequency $\Omega(t) = \frac{E(t)\mu}{\hbar}$

X^+ behaviour

First laser set to X^o (π-pulse)

Electron tunnels out of dot on ~40psec timescale

Hole spin initialised (fidelity ~85%, *recently >99%*[*])

2^{nd} (control) π-pulse creates X^+

With rise-time ~40psec

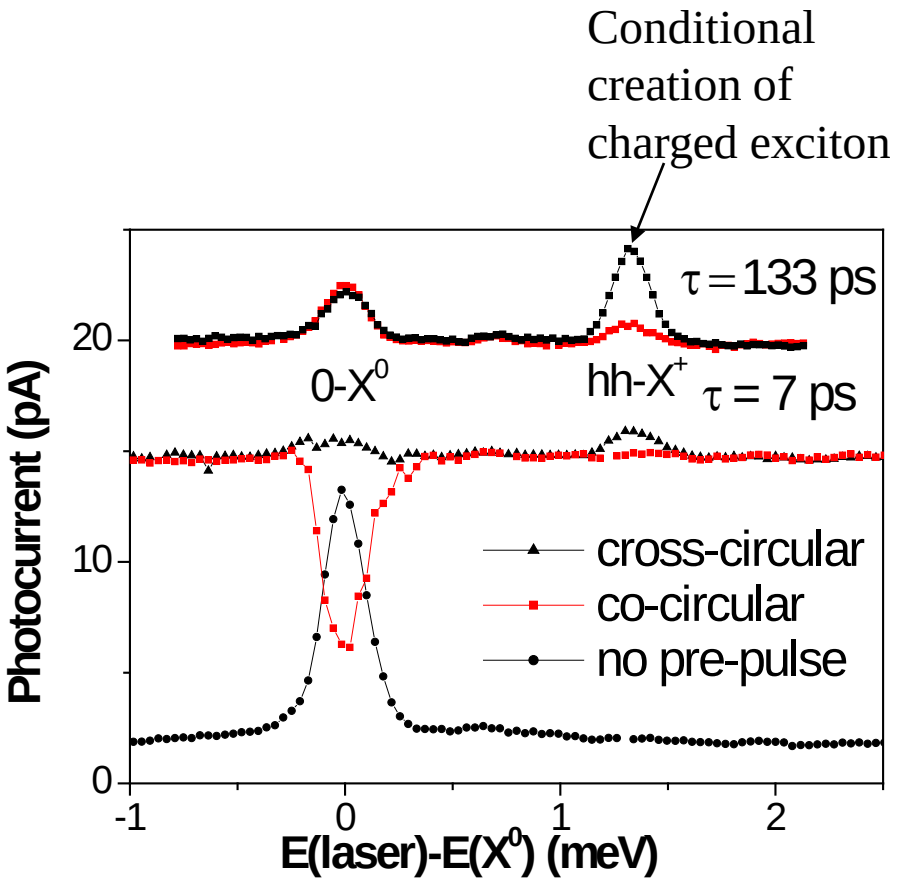

[*]Godden et al, APL in press 2010. Use magnetic field to create pure spin eigenstates. Zeeman splitting >> fine structure spitting.

Time Dependence of X^+ creation and fidelity

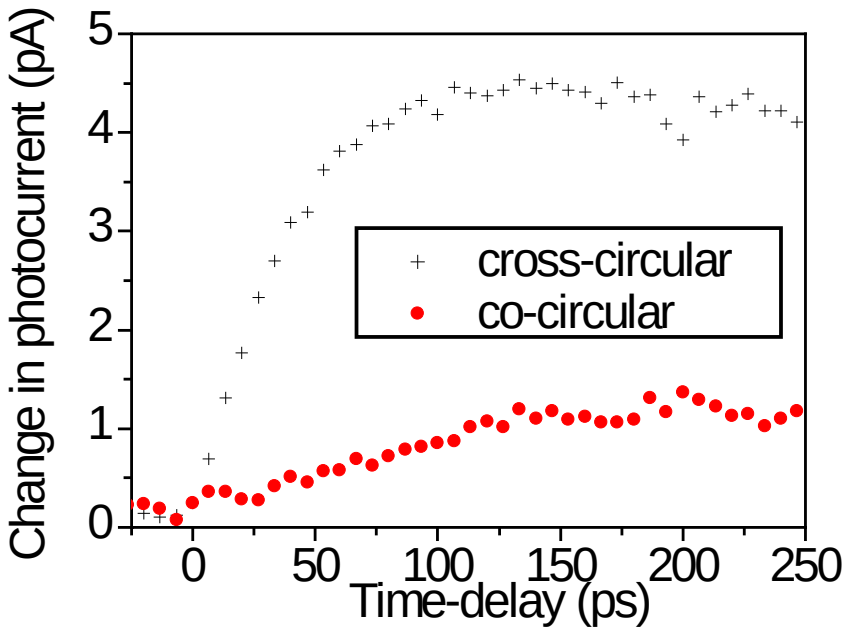

- Rise time of X^+, ~40psec (electron tunnelling time)
- There is signal in co-circular polarisation
- Due to fine structure splitting of X^o which causes precession of exciton spin, timescale ~200psec
- 80% probability of hole occupying correct state
- Is improved in magnetic field to >99% – pure spin eigenstates

High fidelities in magnetic field

Create pure spin eigenstates for $\Delta E_{Zeeman} >> \delta_{fs}$

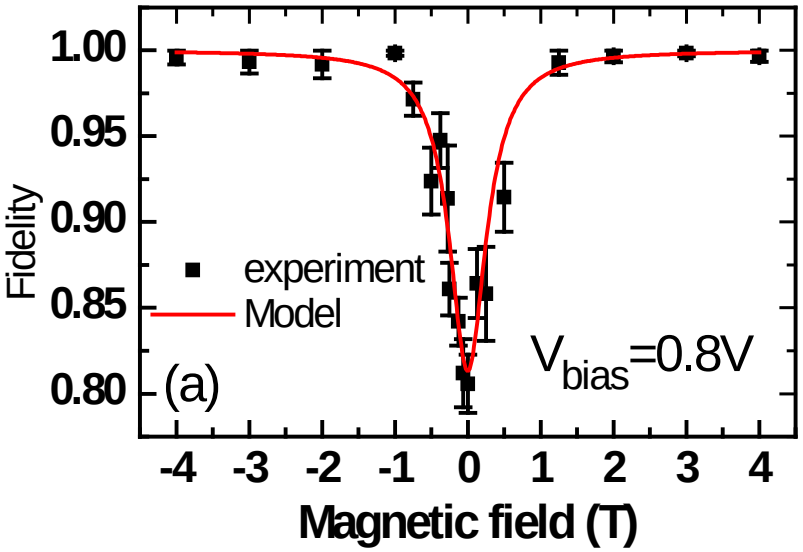

Voltage dependence: fidelity increases with voltage as tunneling time decreases

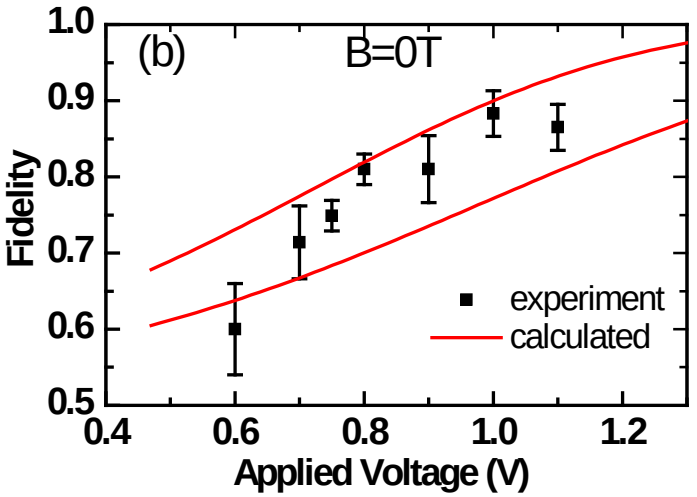

X^o in magnetic field along growth direction (Faraday geometry)

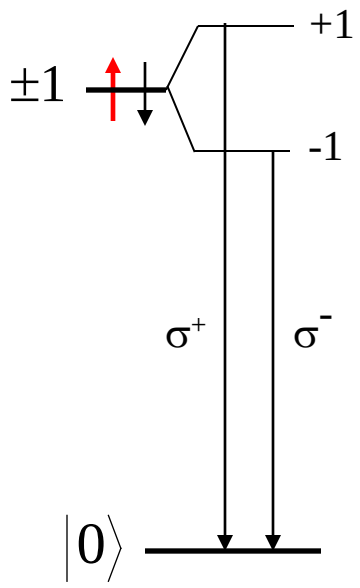

- Splitting into 2 circularly polarised components
- Creates pure spin eigenstates

Control

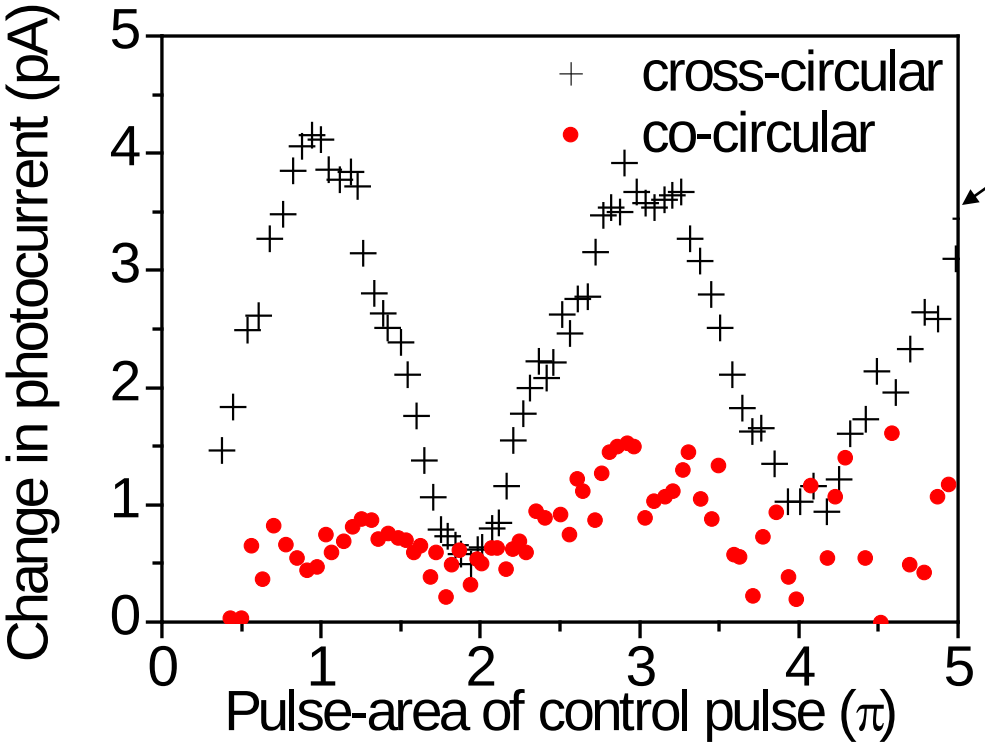

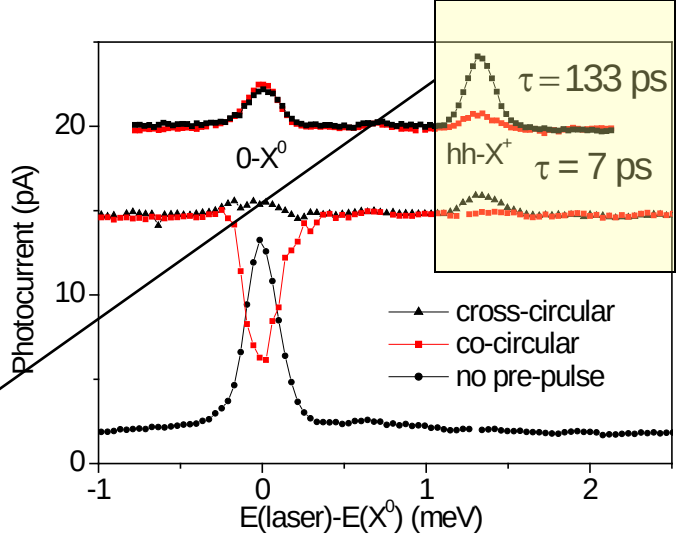

Rabi flop of hh-X^+

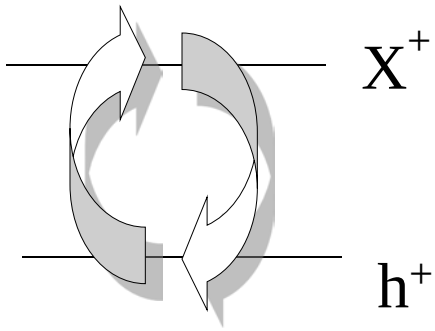

2π pulse brings system back to heavy hole state, but with relative change of phase of π.

Readout: Carriers tunnel out of dot

~nsec timescale (limited by hole – can be longer)

Summary: Part 1

1. Fast initialisation (~50psec)
2. Ultrafast coherent control of single carrier spins. Combine fast speed of exciton manipulation with long coherence of spins.
3. Hole spin to charge conversion
4. Coherence limited by hole tunnelling (fast electrical switching?)
5. Weak hyperfine interaction for holes

2. Controlled Rotation Gate (CROT gate)

Same system as for hole control

Boyle et al, PRB, 075301, 2008

Different spectral range, lower bias

Performed by controlled Rabi rotations on exciton-bi-exciton 2 qubit system.

Previous report for GaAs interface dots

Li et al Science **301** , 809, 2003.

Exciton-biexciton energy levels

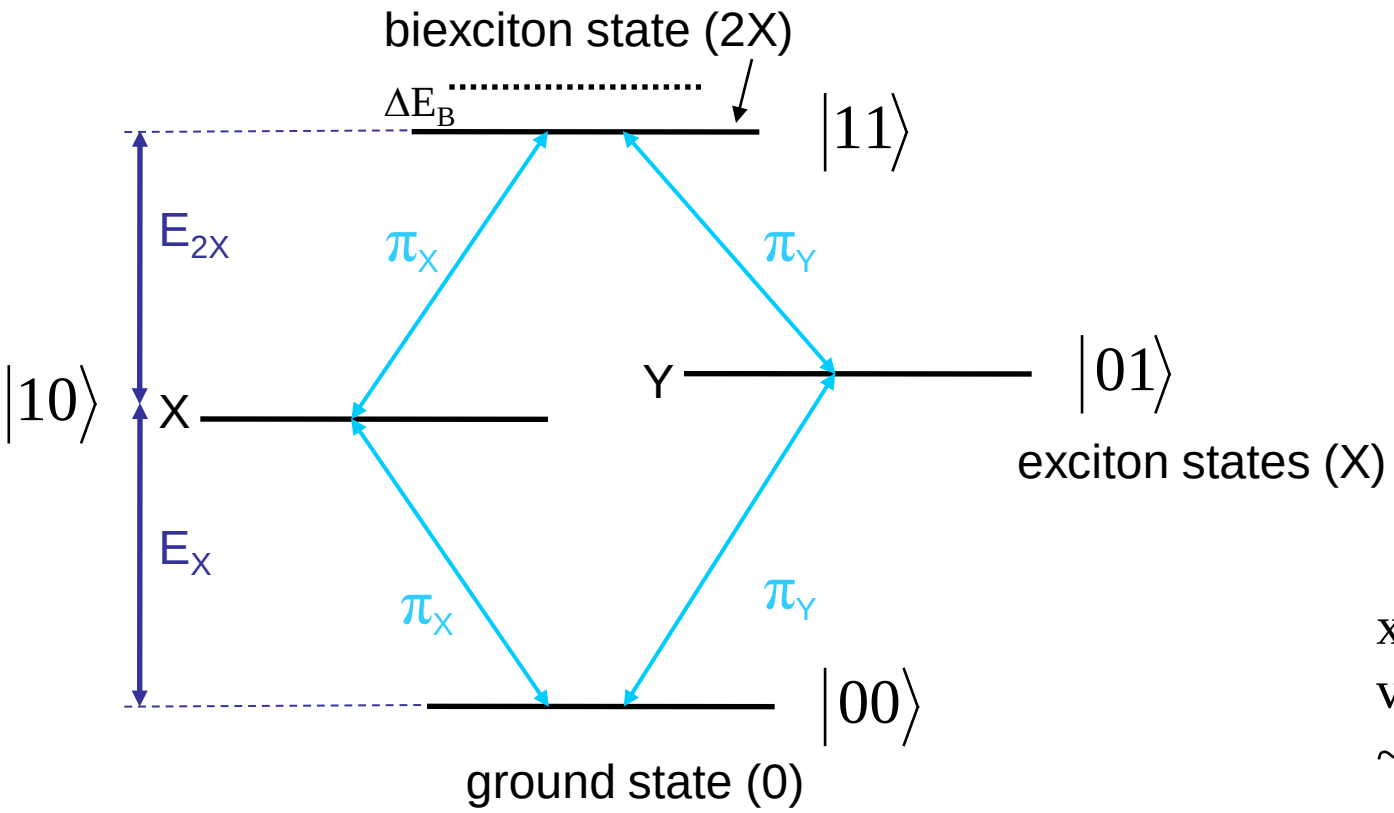

x, y splitting very small ~10μeV

- Encode 2 qubits as the two excitons of exciton-biexciton system
- Polarization and exciton binding energy make transitions spectrally distinguishable. **$E_X - E_{2X} \sim 2.4$meV**
- 0,1 label absence or presence of exciton

C-rot gate: Principle of Operation

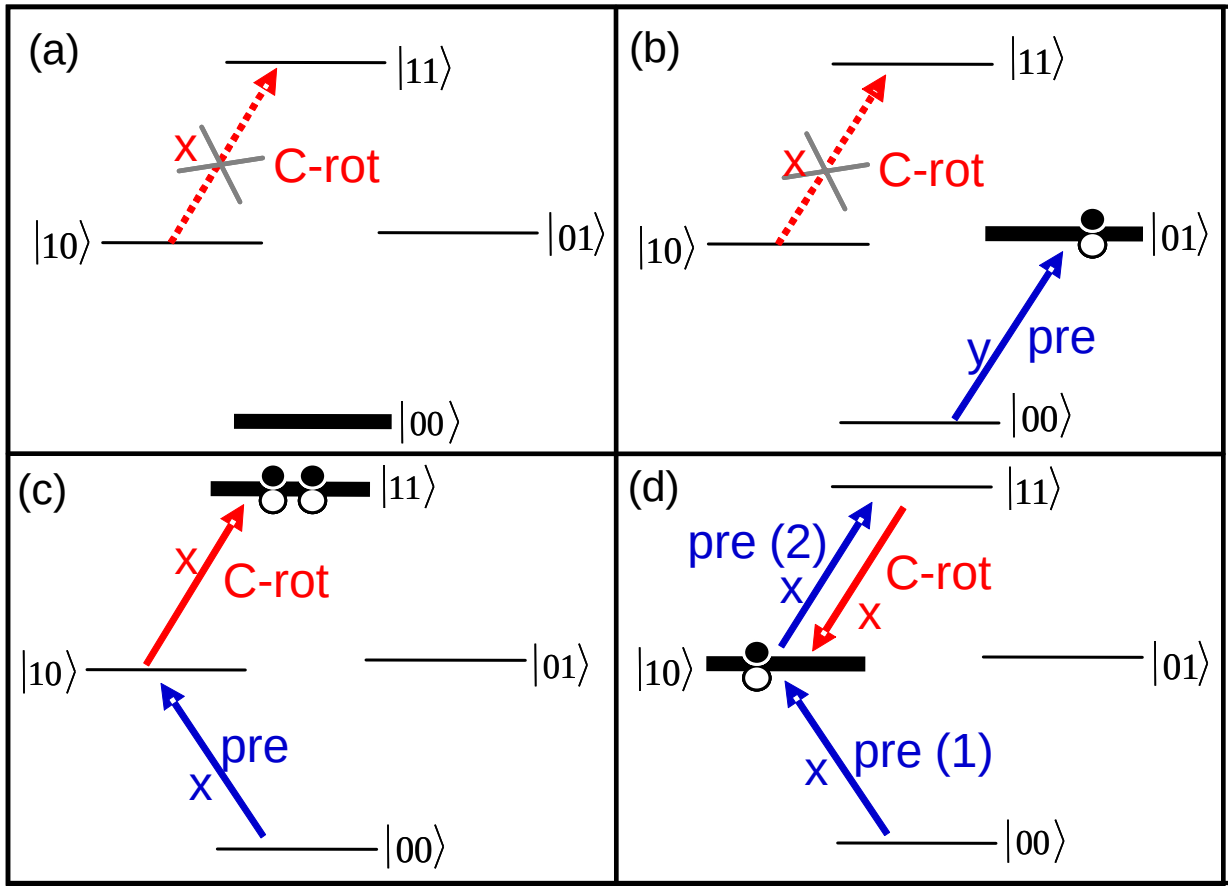

(a) $U_{CROT}|00\rangle = |00\rangle$

(b) $U_{CROT}|01\rangle = |01\rangle$

(c) $U_{CROT}|10\rangle = i|11\rangle$

(d) $U_{CROT}|11\rangle = i|10\rangle$

Flips state of 'target' qubit if 'control' qubit is in state '1'

Conditional logic

- C-rot π pulse only interacts when the initial state of the dot is $|10\rangle$ or $|11\rangle$

$$E_{pre} - E_{C\text{-}rot} \sim 2meV$$

First π-pulse set to create X^o

Second π-pulse creates bi-exciton

Strong selection rule for bi-exciton creation

Co-linearly polarised (i.e. x-x or y-y)

X^o-$2X^o$ creation conditional on X^o pre-pulse

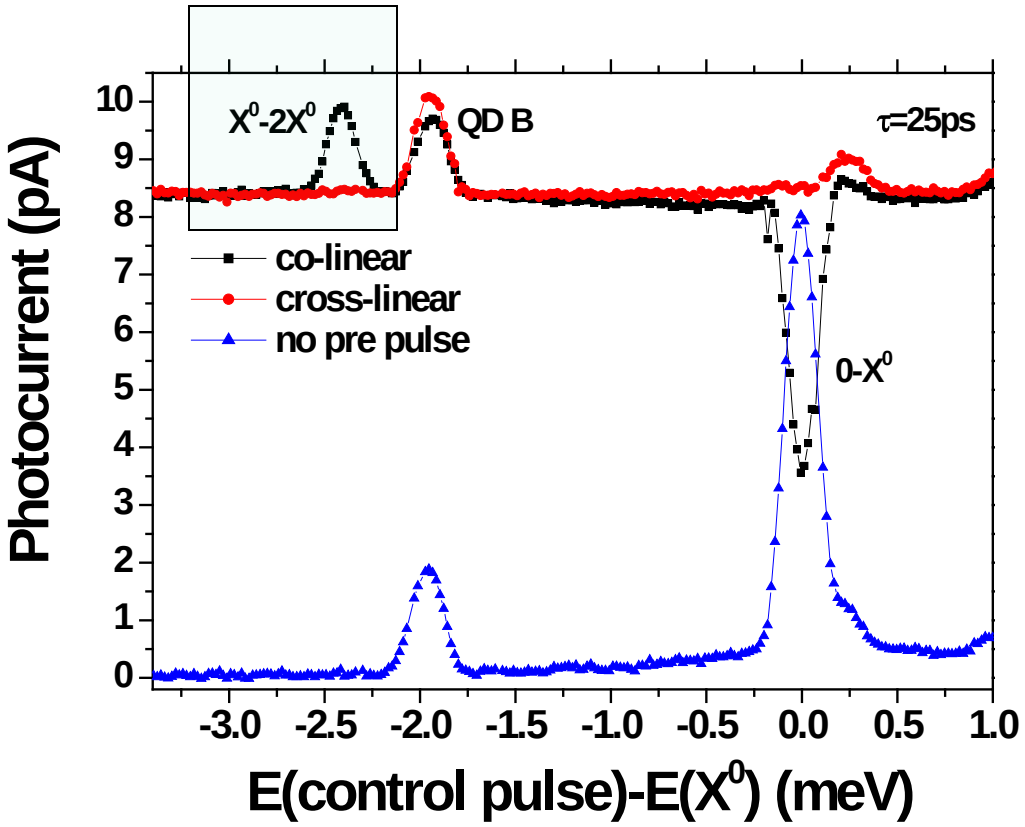

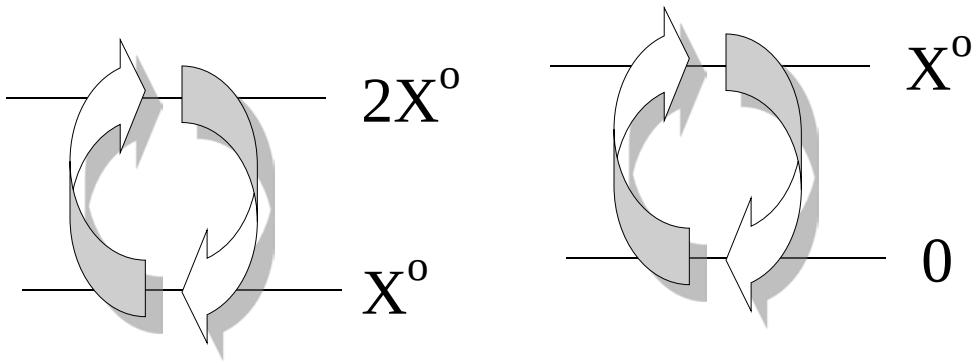

X-2X Rabi oscillations

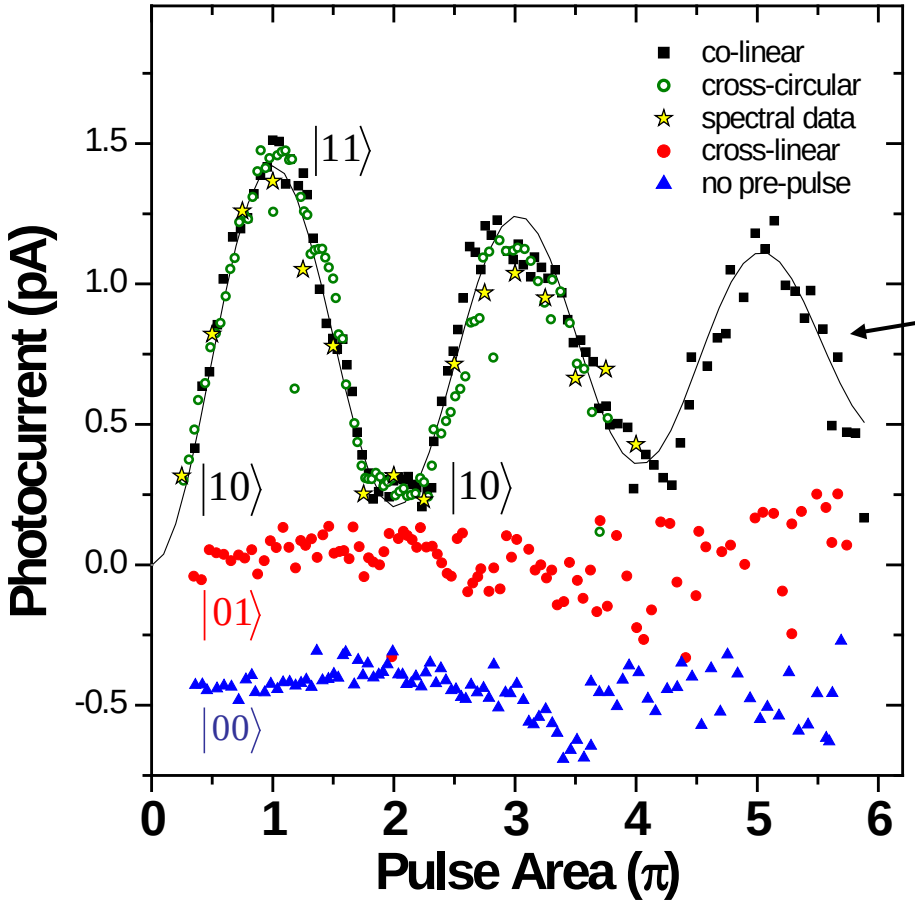

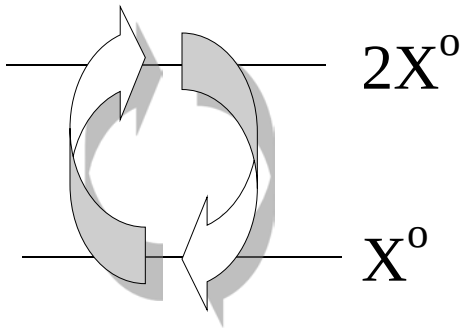

First pulse (pre-pulse) tuned to $X^o \rightarrow |10\rangle$

Then second co-polarised pulse creates $|11\rangle$ Rabi flops

C-NOT	
$\|00\rangle$ ⇨	$\|00\rangle$
$\|01\rangle$ ⇨	$\|01\rangle$
$\|10\rangle$ ⇨	$\|11\rangle$
$\|11\rangle$ ⇨	$\|10\rangle$

>10 operations before loss of coherence, >50 possible

Part 2: Summary

- Observation of conditional Rabi rotation of exciton-biexciton transition
- >50 operations before within coherence time
- Potential high fidelity, but scalability difficult

3. Dressed states (exciton-photon coupled states) (polariton formation)

- Interaction of two level atom with photon field
- Observation of Rabi oscillations in time domain

Boyle et al, PRL 102, 207401 (2009)

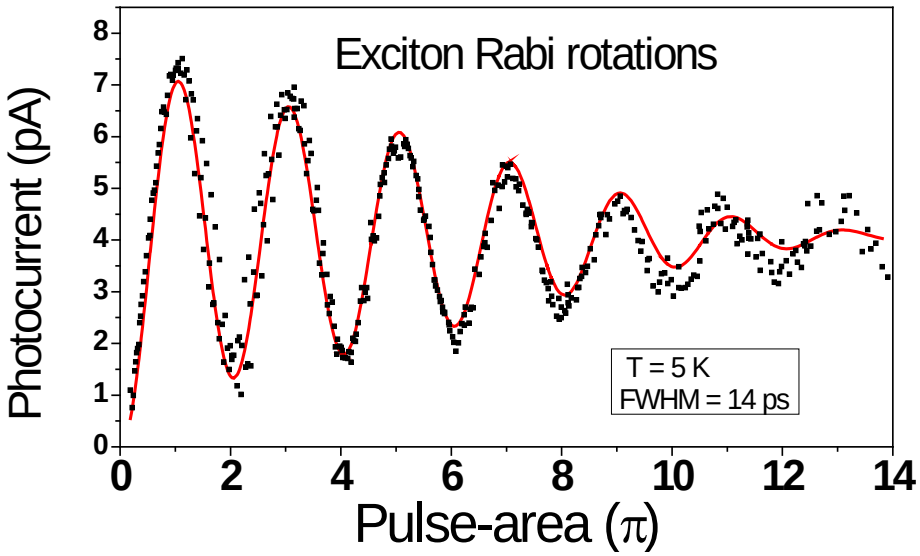

<u>Continuous wave observations of dressed states</u>

absorption: Xu et al Science 2007, Kroner APL 2007, Jundt et al, PRL 2008, Gerardot et al 2009

emission: Kamada PRL 2001, Muller, Solomon PRL 2008, Flagg Nat Phys 2009

Bare states Dressed states

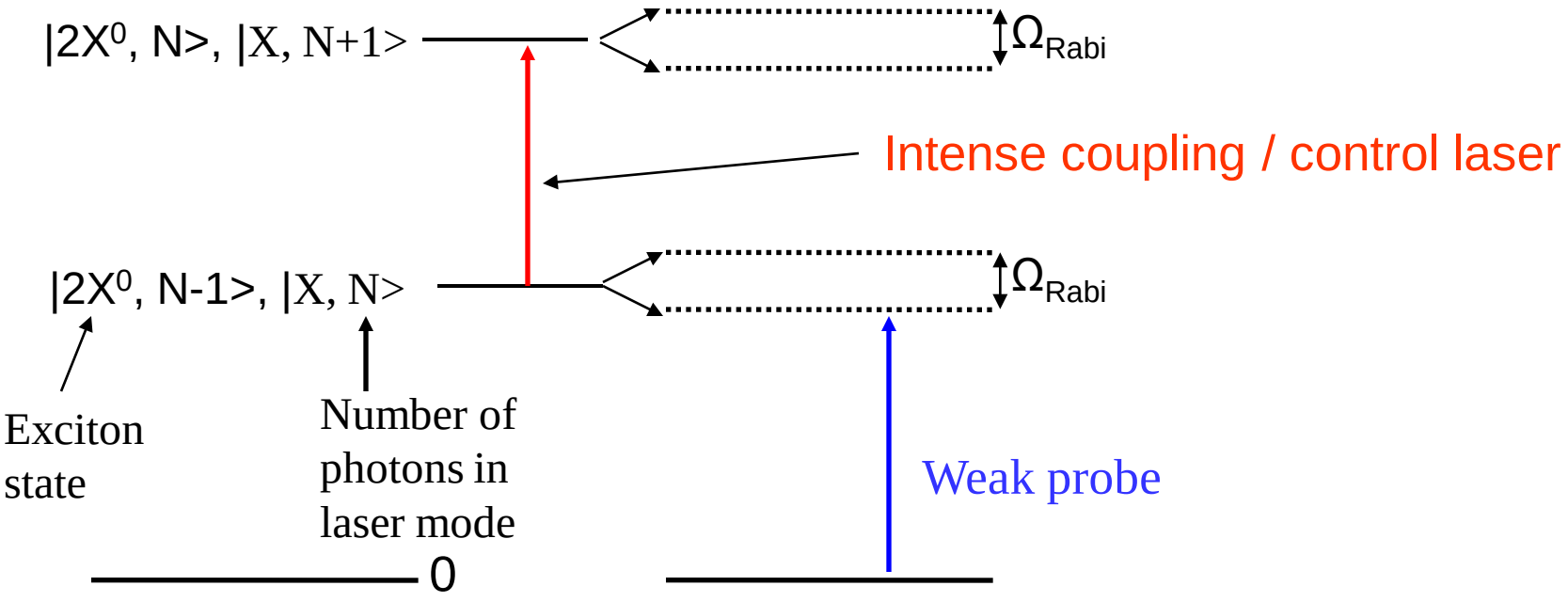

Control laser resonant with X^0-$2X^0$ transition creates dressed states split by Rabi frequency Ω_{Rabi}.

Dressing of exciton-biexciton states

Optical coupling of exciton and biexciton states forms a pair of dressed states, observed as an Autler-Townes doublet (X-2X energy separation ~2meV)

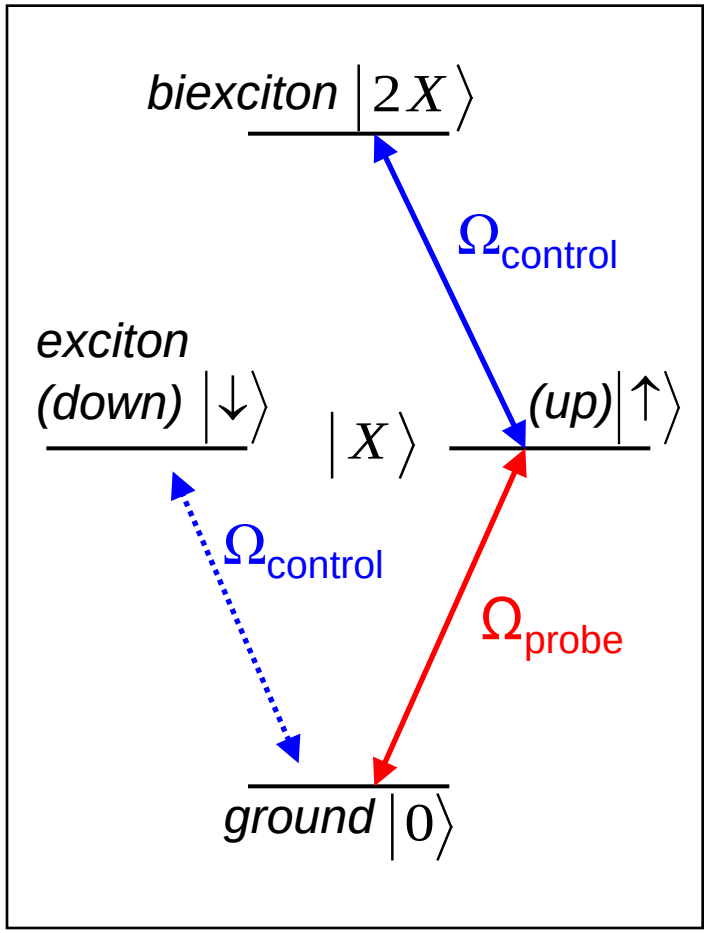

Exciton-biexciton system

Power dependent splitting

Experiment

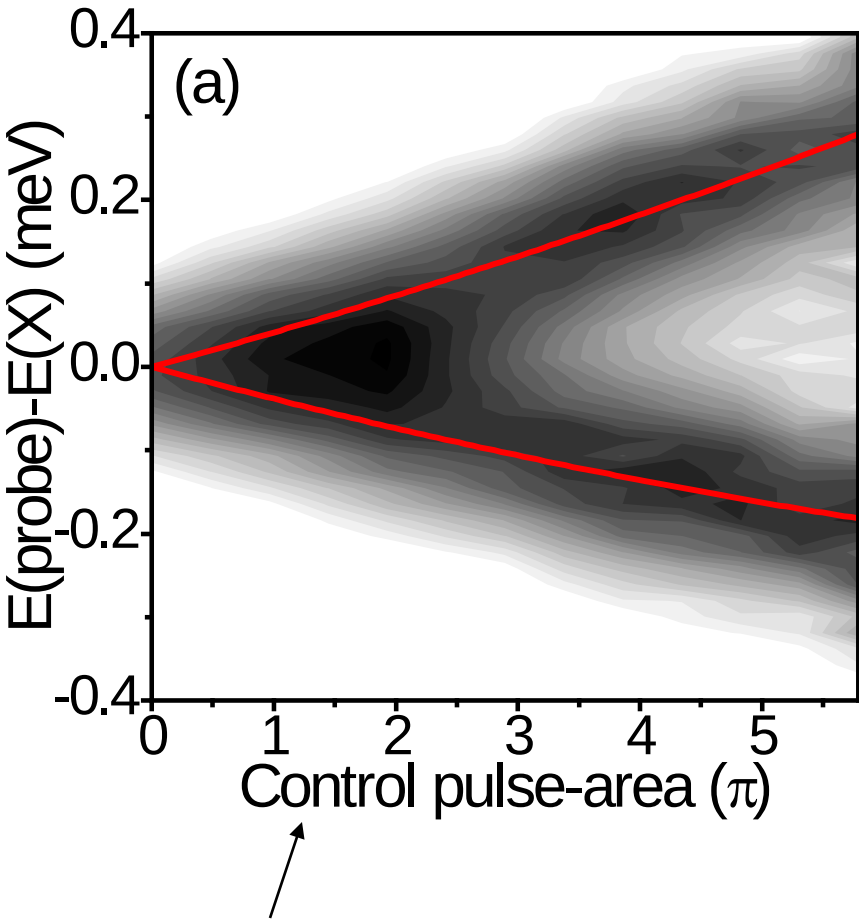

Calibrated from Rabi flops

Very large splitting ~450μeV due to high peak power (2meV later)

Theory

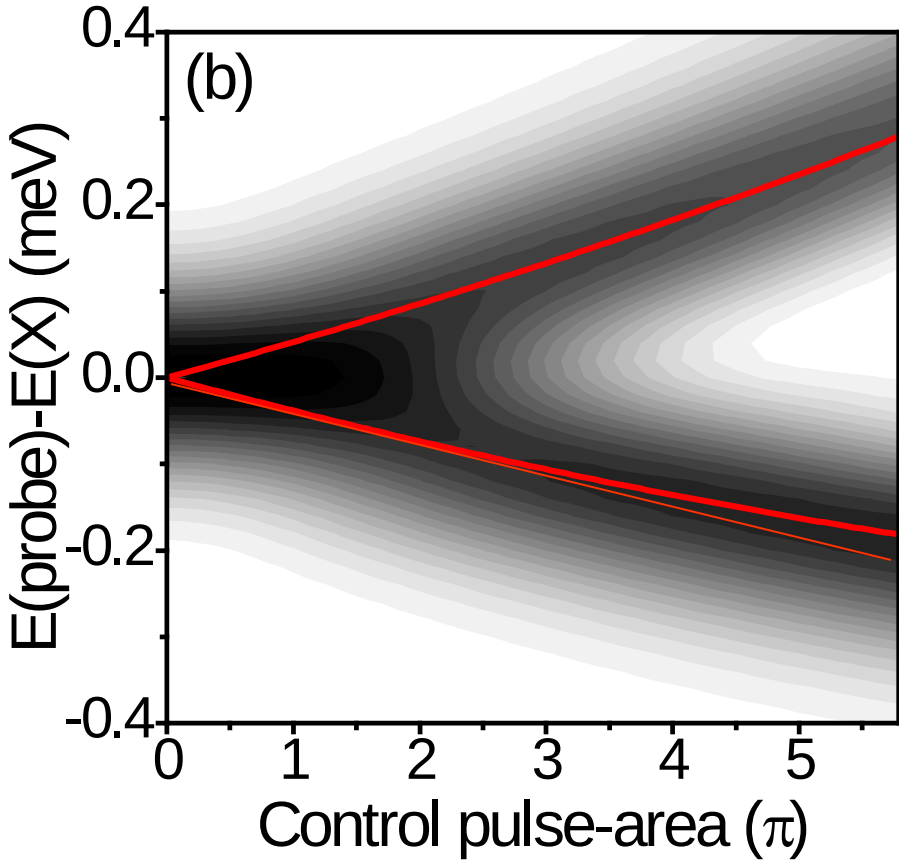

Splitting A-T spitting of dressed states

Non-linear shift: ac Stark effect

Anti-crossing of dressed states

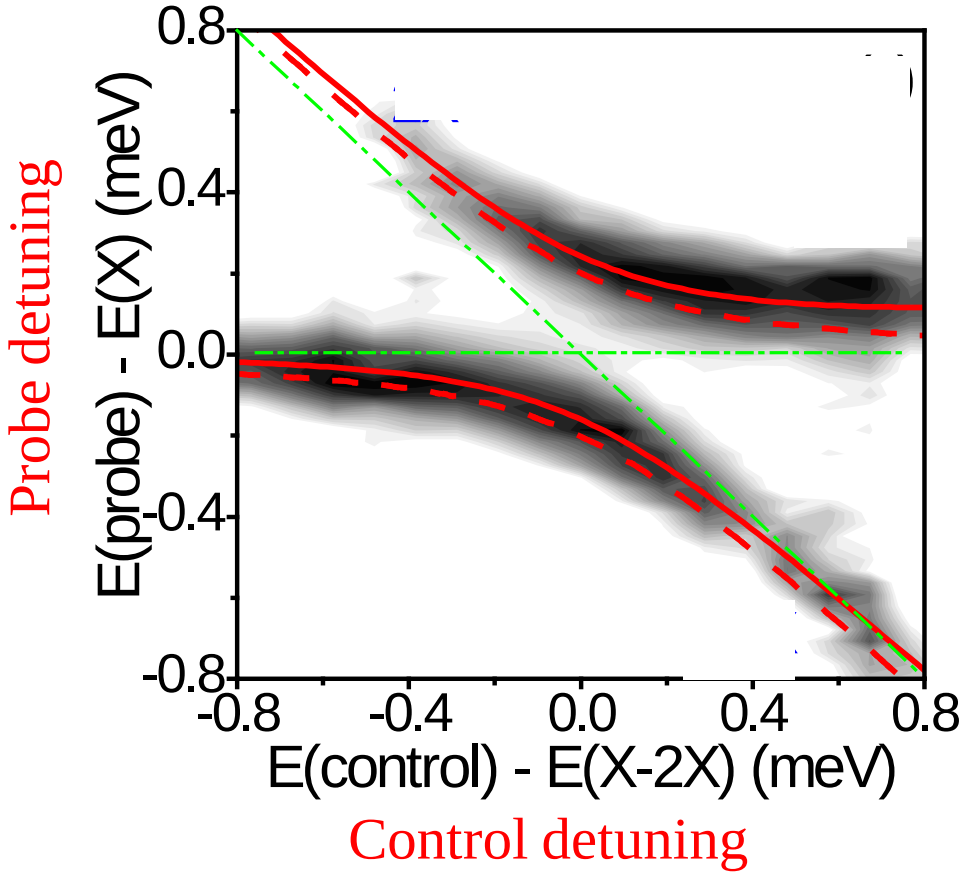

$$\Delta E(\pm) = \left(-\delta_c \pm \sqrt{\delta_c^2 + \Omega_R^2} \right)$$

Time evolution of splitting

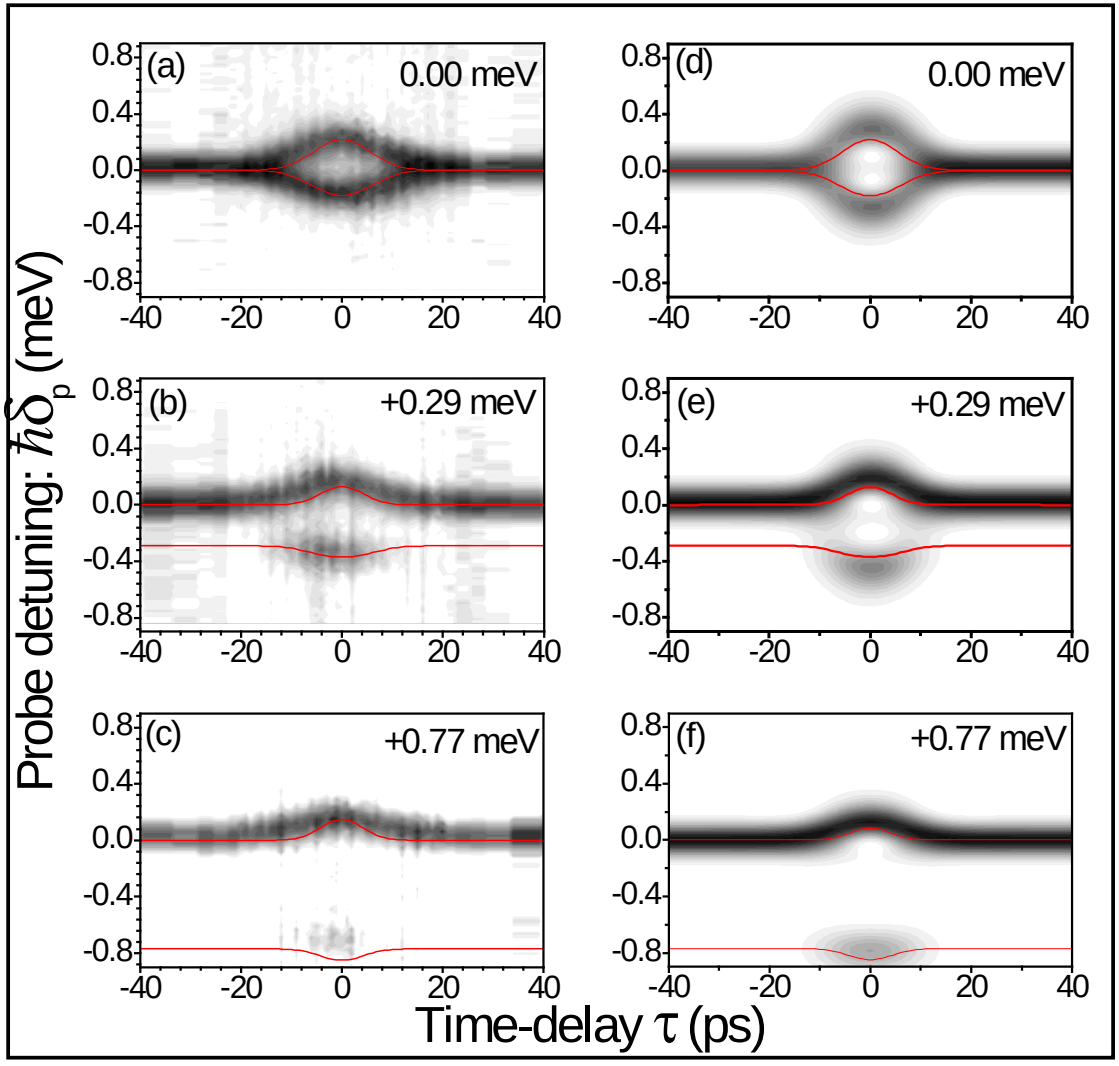

Splitting follows the control pulse

⇒ Coherent effect (i.e. no field, no splitting)

⇒ Not a result of carrier nonlinearity

⇒ We can manipulate the Rabi splitting, and the dressed states on picosecond timescales. (‘adiabatic control’)

Time resolution of Rabi oscillations

- **Use a spectrally broad, temporally short probe pulse, and a long control pulse to time-resolve the Rabi oscillations.**

- **The Rabi oscillation is the signature of Rabi-split dressed states in the time domain.**

For QWs, Schulzgen, *Phys. Rev. Lett. 1999*

Rabi oscillations in the time domain

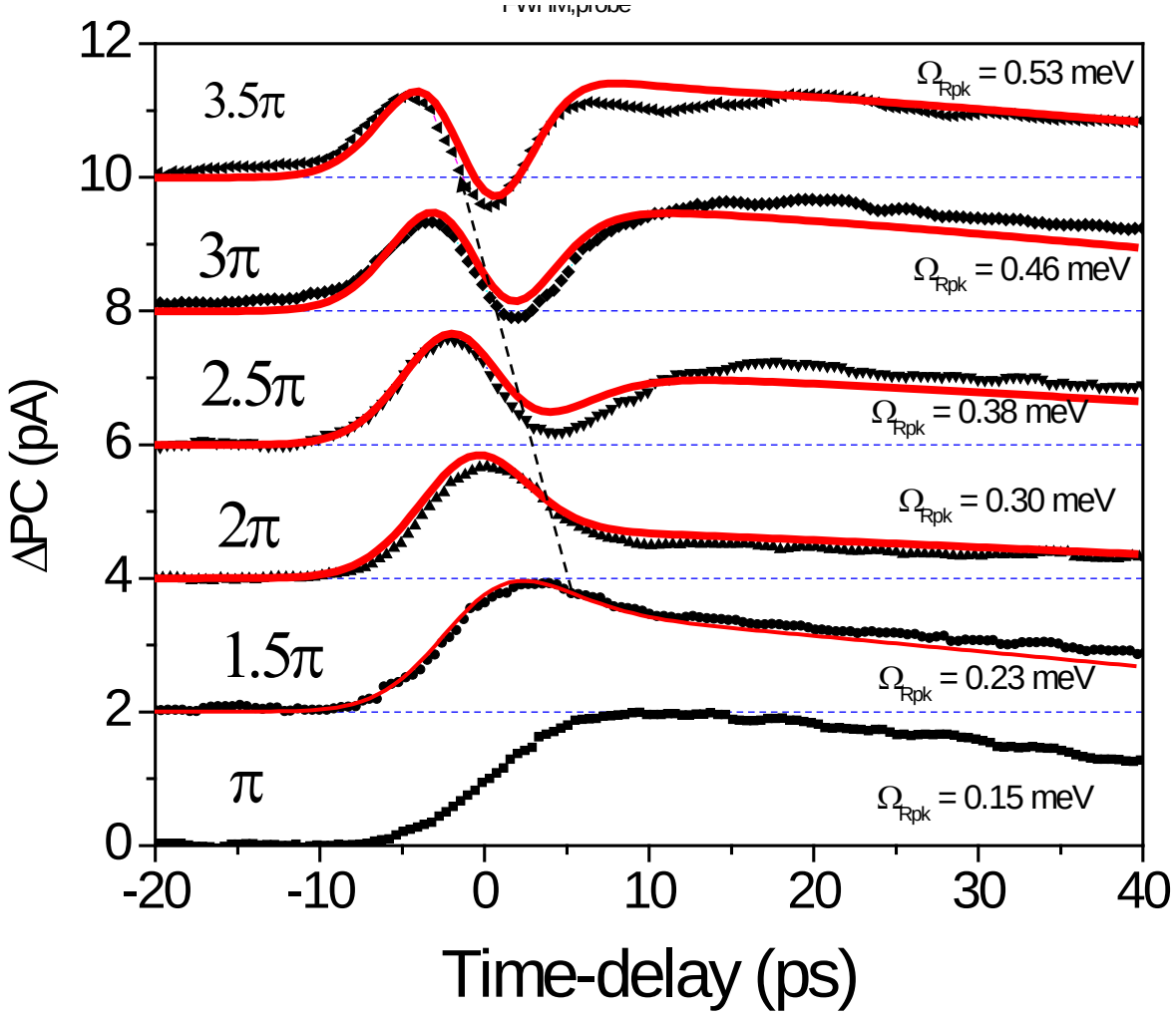

- Oscillation frequency increases with pulse area: increasing Rabi frequency
- Ultrafast gating of dressed states

Control 10ps, probe 3ps. Positive delay, control follows probe.

Part 3: Summary

- An intense laser pulse couples the exciton and biexciton states
- Observe beat between X/2X dressed states, time-resolving the X-2X Rabi oscillation
- Creation of coherent superposition of dressed states and control of their relative phase

Part 4: Excitation induced dephasing and its wider significance (intensity damping)

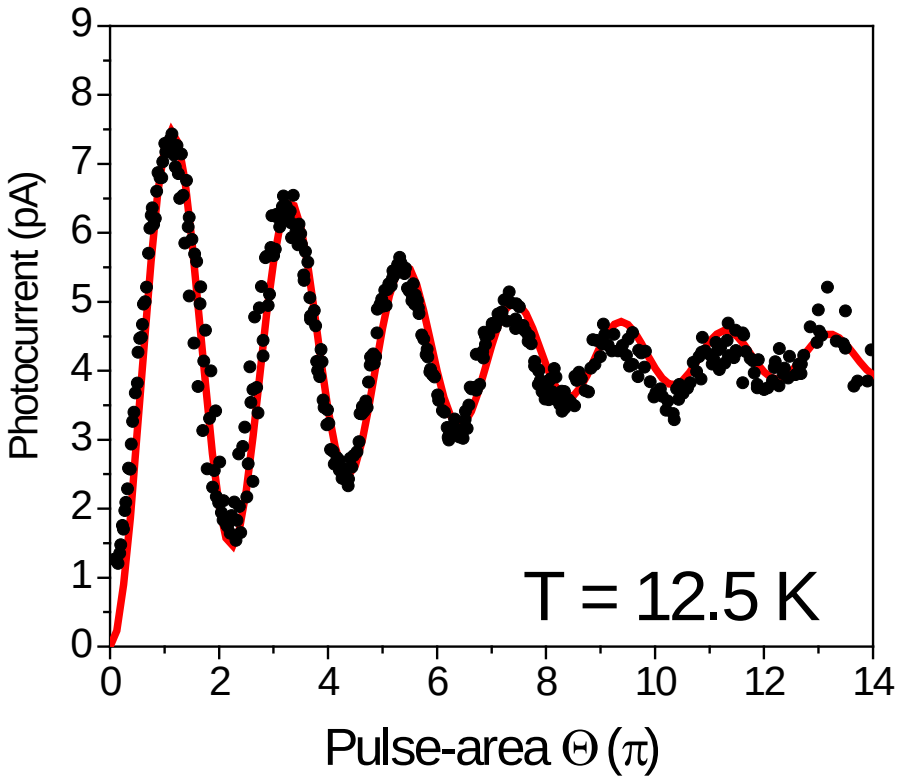

Ramsay, PRL 104, 017402, 2010
and arxiv 1005.1580

- 2 level system coupled to bath of bosons
- Real and imaginary parts of response function
- Damping of Rabi rotations with increasing pulse area
- Analogy with Lamb shift
- Study temperature dependence to determine mechanism

Possible mechanisms

(i) Acoustic phonons (intrinsic) : $\lim_{\Omega \to 0} \Gamma_2 \propto T\Omega^2$ [A. J. Leggett, Rev. Mod. Phys. 59 1 (1987).]

(ii) Wetting layer (p-shell): $\Gamma_2 \propto \Omega^2$ [Q. Q. Wang, PRB 72 035306 (2005)]

(iii) Multi-exciton effects (broadband excitation) [B. Patton PRL 95 266401 (2005)]

Physical origin of damping

As system driven harder, Rabi energy increases (up to ~2meV), coupling to larger density of phonon states

In presence of strong optical field, states are dressed (*Boyle et al, PRL 102, 207401 (2009)*

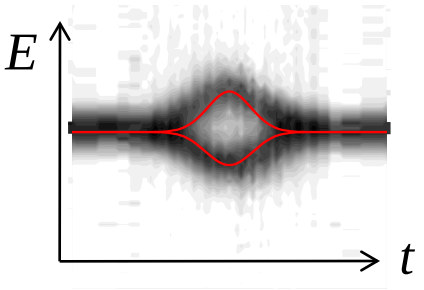

Damping arises from acoustic phonon scattering between dressed states

Previous theory work: Nazir PRB 78 153309 (2008), Vagov PRL 98, 227403, 2007, Förstner et al PRL 91, 127401, 2003, Krügel et al, PRB 73, 035302, 2006

Exciton two level system coupled to phonon bath

$$H_I = |X\rangle\langle X| \sum_{\mathbf{q}} \hbar \left(g_{\mathbf{q}} b_{\mathbf{q}}^{\dagger} + g_{\mathbf{q}}^{*} b_{\mathbf{q}} \right)$$

Optical Bloch equations, model [A. Nazir PRB 78 153309 (2008)], Markovian approximation, second order perturbation theory

Rabi frequency dependent pure dephasing

$$\frac{\partial s_2}{\partial t} = [\Omega(t) + \Im[K(\Omega)]]s_3 - [\Gamma_2^{*} + \Re[K(\Omega(t))]]s_2$$

Shift to Rabi rotation frequency

$$\frac{\partial s_3}{\partial t} = -\Omega(t)s_2$$

Note real and imaginary parts – related by Kramers-Kronig relation

Example of Rabi rotation in high driving-field regime (comparison to Ω^2 – damping)

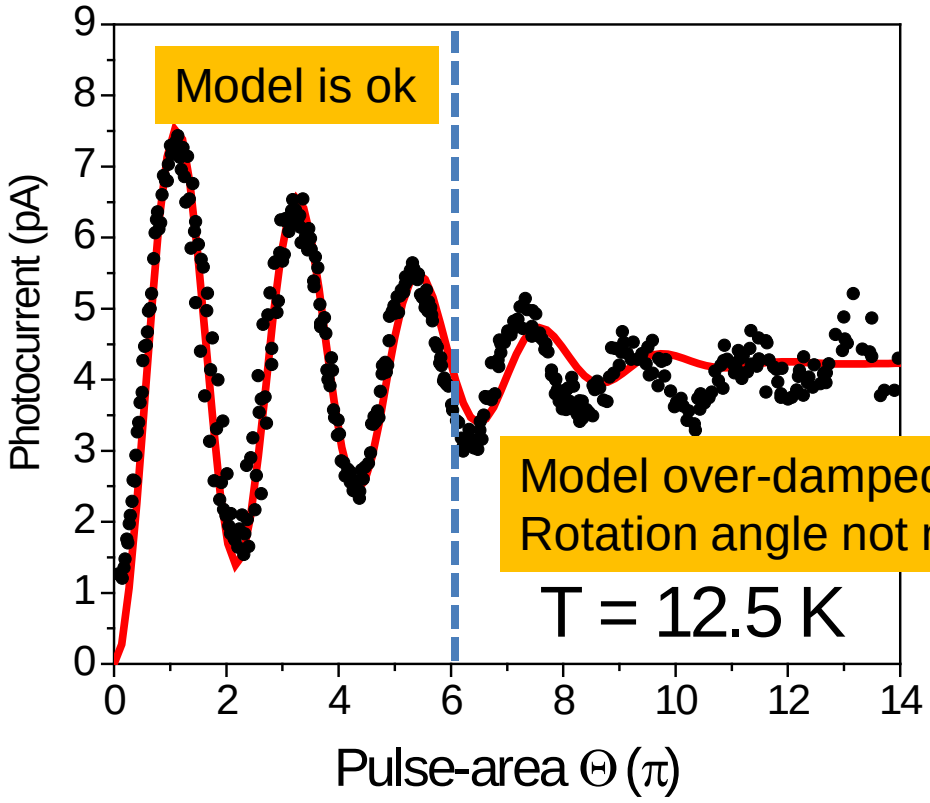

To leading order in the Rabi frequency Ω_R the rate of dephasing is: $\Gamma_2 = K_2\Omega_R^2$

Include the exciton-phonon form-factor
$P(\omega) \approx \exp(-\omega^2/2\omega_c^2)$

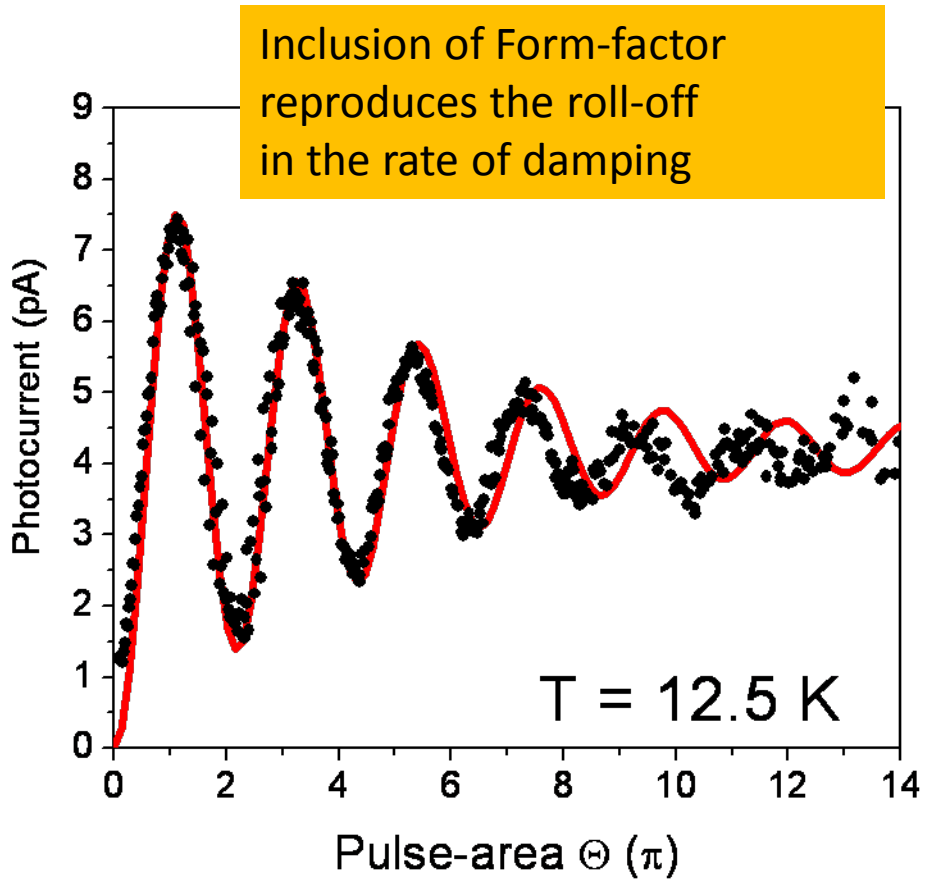

Against the periodic signal of the red-line,
The rotation angle is clearly a nonlinear function of the driving-field
$\Rightarrow$Shift to effective Rabi rotation frequency

Coherence revivals?? (Vagov et al, PRL98, 227403, 2007)

Include both real and imaginary parts of exciton-phonon response K(Ω), to satisfy Kramers-Kronig relationship

Non-monotonic decay, and nonlinearity of the rotation angle described by same function K(t)

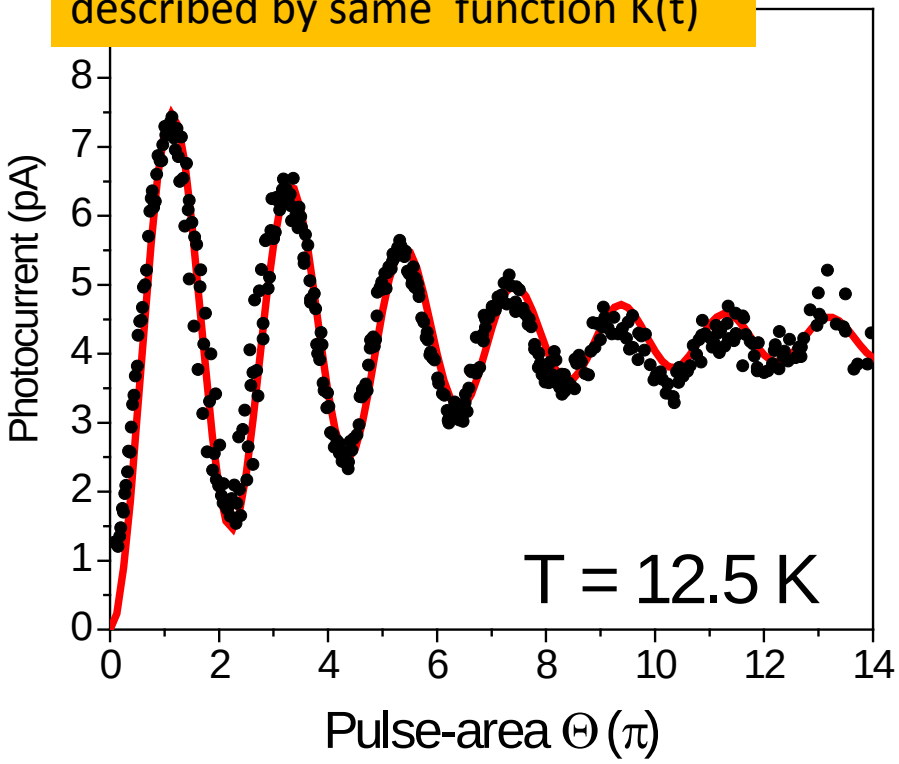

$K_2 = AT$; A= 11.2 fs/K
$\Gamma_2^* = 0.025$ 1/ps
$\hbar\omega_c = 1.44$ meV

Study Rabi oscillations as a function of temperature to determine mechanism of damping

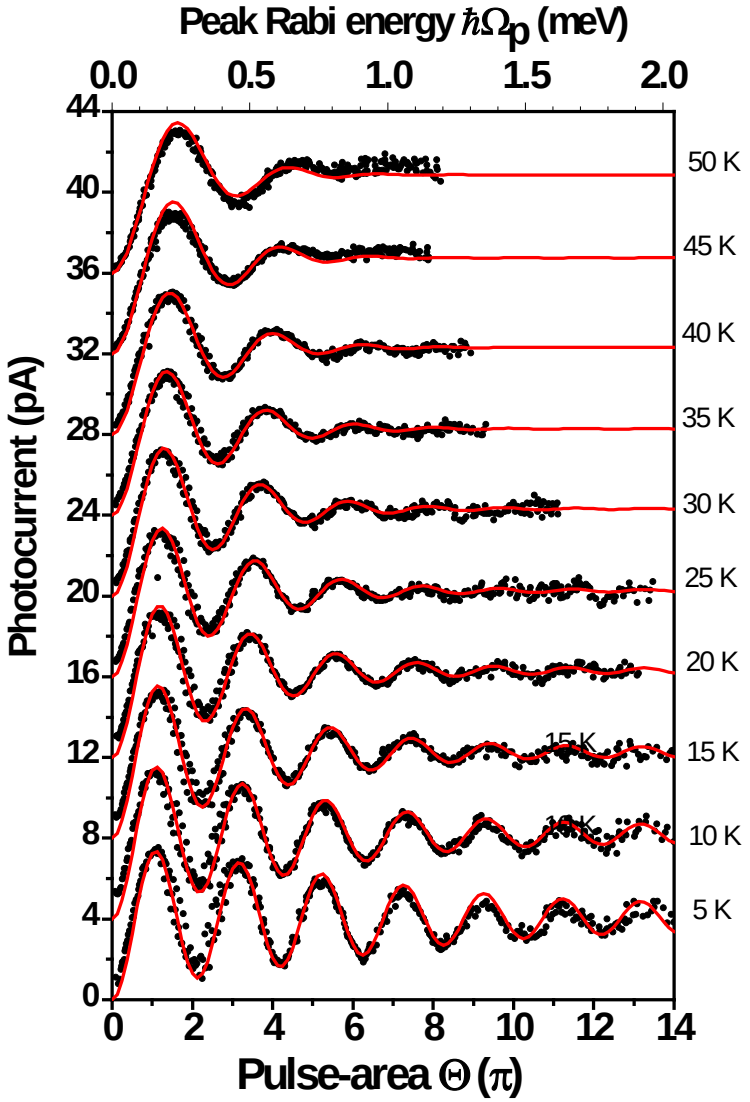

- Strong increase of damping with temperature
- Due to coupling of exciton states to acoustic phonons (3D boson bath)
- Good global fits obtained
- Excitation induced dephasing is an intrinsic feature of the solid state environment of QD two level qubits

Temperature dependence of photocurrent spectra

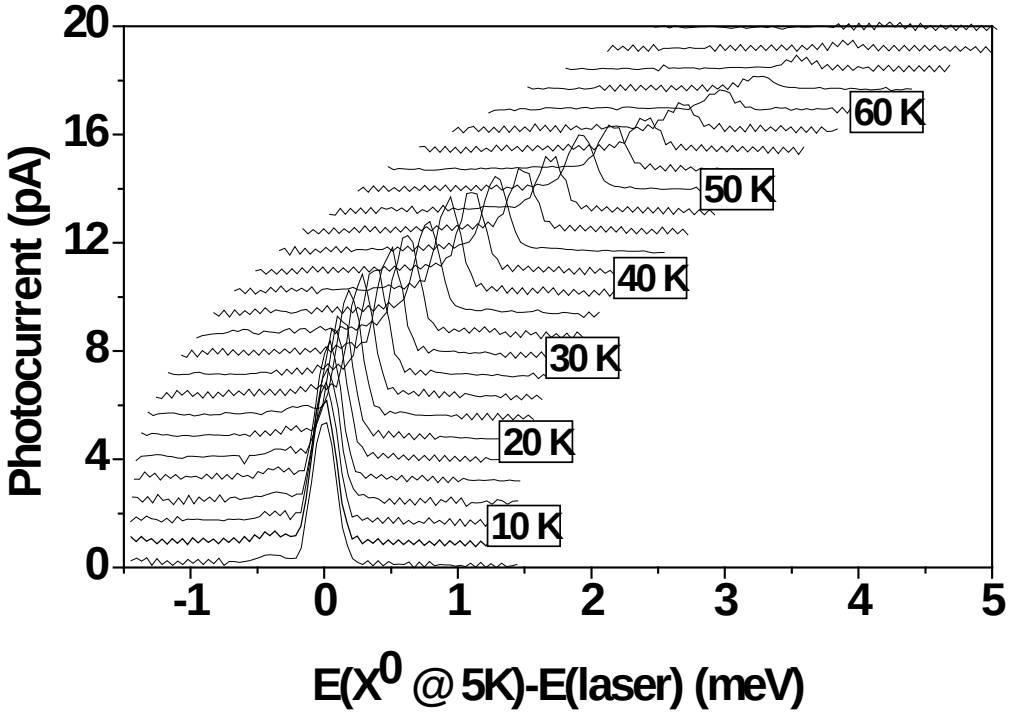

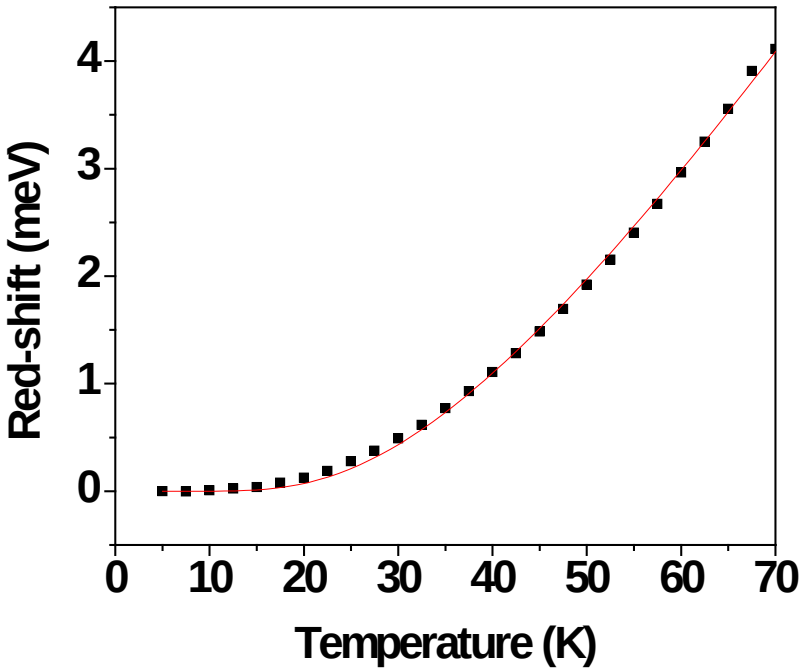

Laser retuned at each temperature for Rabi flops

Linear temperature dependence of excitation induced dephasing time ⇒ Acoustic phonon model

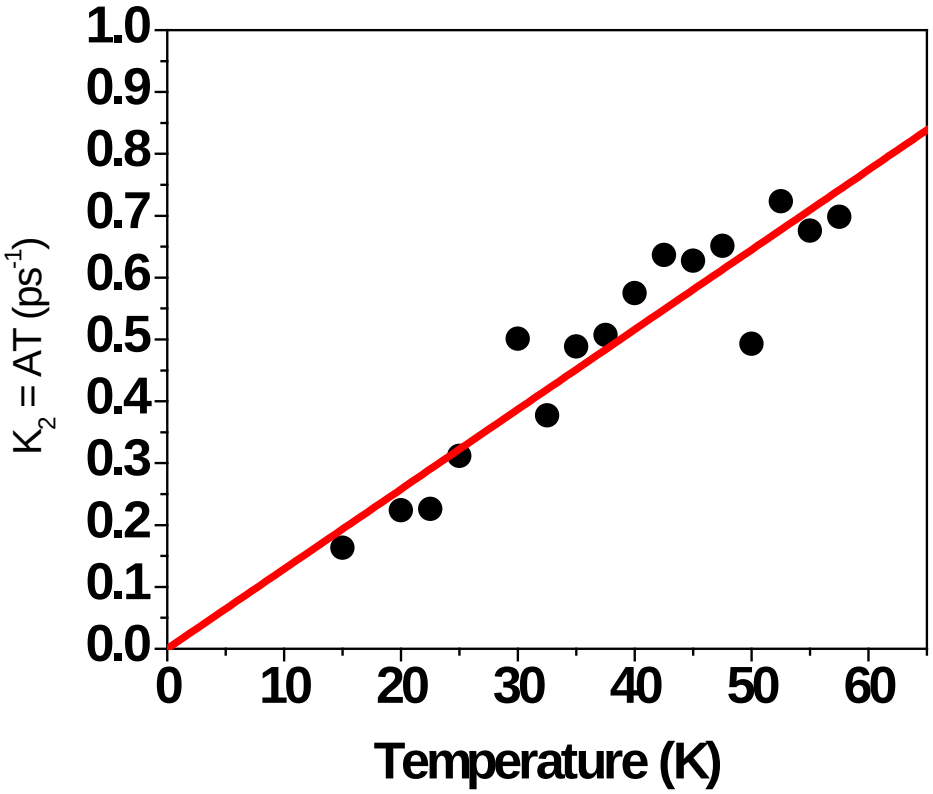

Damping rate

$\Gamma_2 = AT\Omega^2 = K_2\Omega^2$

Shows linear dependence, with magnitude close to that predicted by theory, with known values of deformation potential constants

$$K_2 = \frac{(D_e - D_h)^2}{4\pi\mu c_s^5\hbar^2} k_B T \equiv AT.$$

Theory: E. M. Gauger, B. W. Lovett, Oxford, A. Nazir, UCL

Fitting procedure

Five experimental features: period, amplitude, strength of damping, cut-off in damping, non-linearity of period

Four parameters:

A, $\hbar\omega_{cut\text{-}off}$, global values to fit all temperatures

a, the pulse area axis, and η amplitude of oscillations

Temperature dependence of period provides further test of consistency

$$K_2 = \frac{(D_e - D_h)^2}{4\pi\mu c_s^5 \hbar^2} k_B T \equiv AT.$$

Temperature dependence

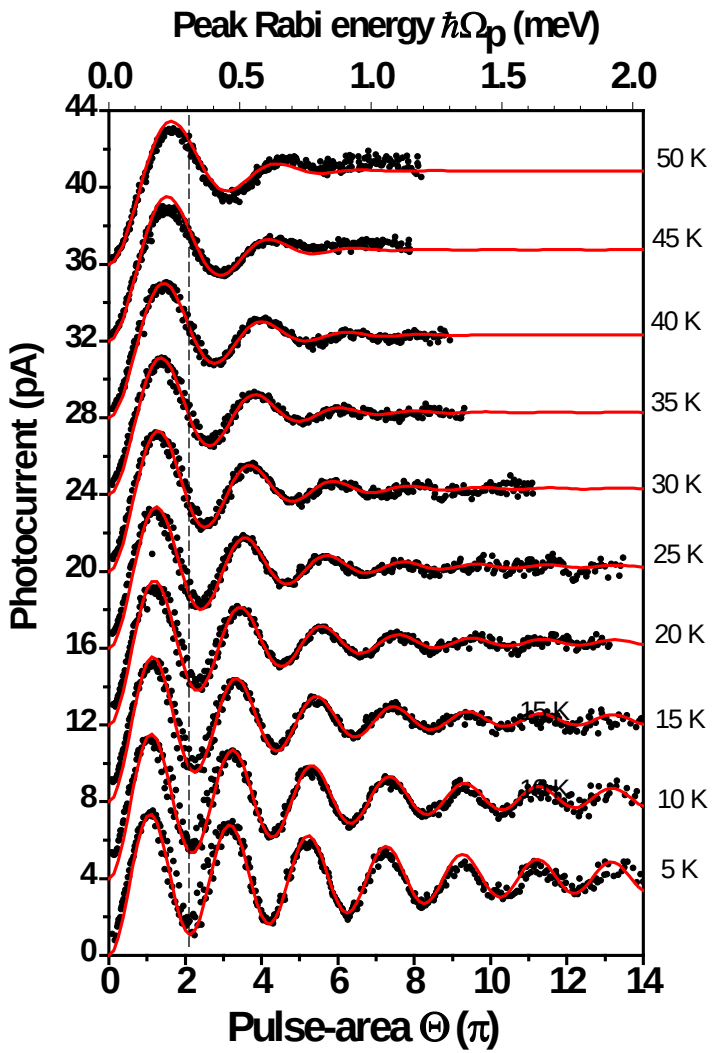

see arxiv 1005.1580

- Shift of frequency with temperature
- Decrease of period with pulse area
- Arise from imaginary part of response function (changes in real part leading to damping)
- Related by Kramers-Kronig relation
- Analogous to Lamb shift for atoms (shift of atomic energy level due to fluctuations in vacuum field – quantum electrodynamics)
- Here we deal with fluctuations in 3D phonon field

Temperature dependent ‘period’

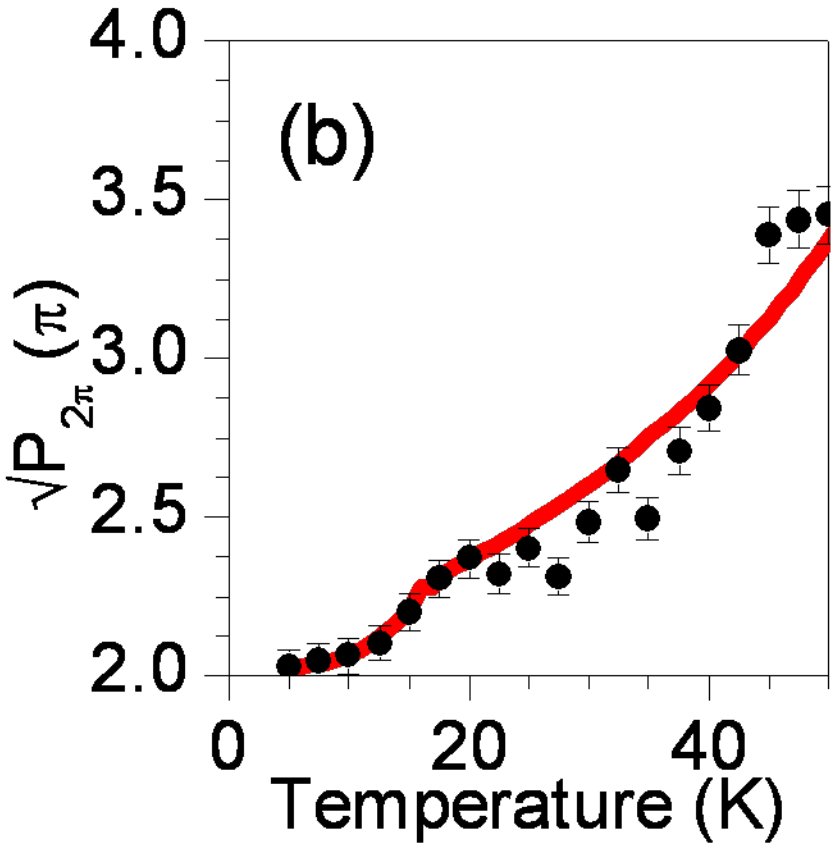

Good agreement between full theory and experiment

Temperature independent coupling of dot to laser field

Provides further confidence in model

Lamb shift in atomic physics

- Radiative shift and broadening of 2s state of hydrogen atom caused by coupling to fluctuations of vacuum field

- Vacuum fluctuations cause electrons to vibrate

- Averages Coulomb field over distance and hence **shifts** energy

- Spontaneous emission, stimulated by fluctuations in vacuum field, causes **broadening**

Exciton-phonon case

Exciton two level system couples to fluctuations of phonon field

Extrapolation to zero temperature gives true analogy with Lamb shift

With increasing temperature, increase phonon population, hence increasing shift

Analogy with driven case in optics – the a.c. Stark effect

Zero temperature shift to Rabi-energy: “Phonon-induced Lamb-shift”

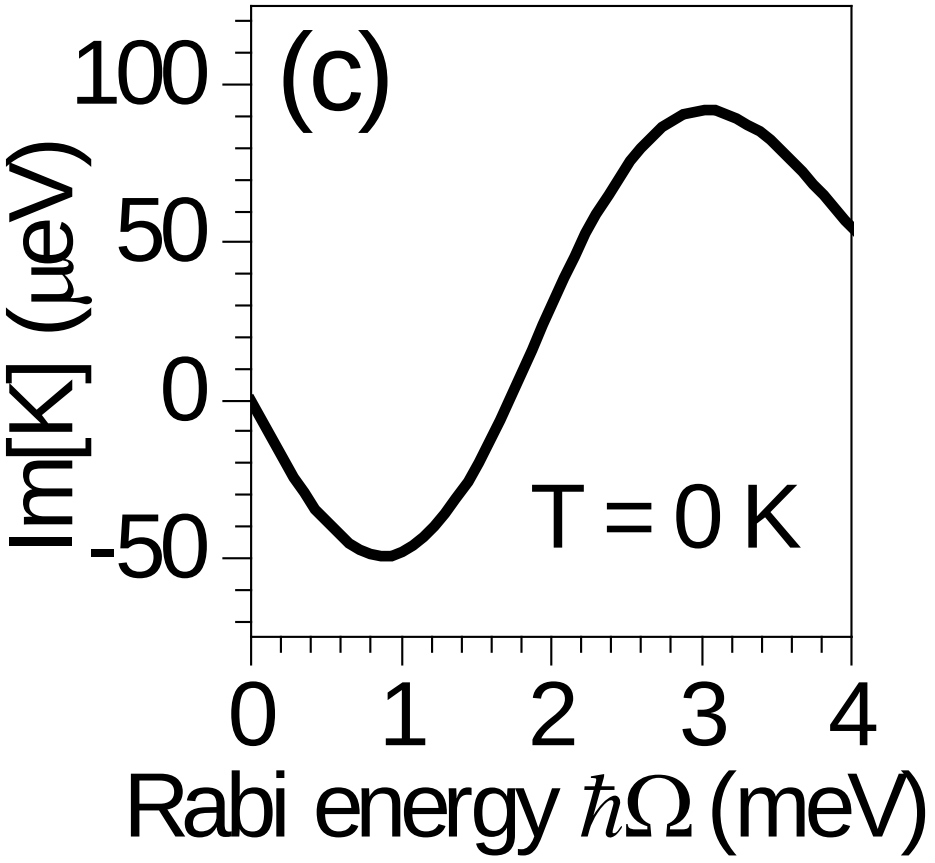

Shift at first minimum is ~50μeV (5%)

Summary Part 4

- Excitation induced dephasing due to coupling to LA phonons
- Such dephasing is probably fundamental feature of optical control of exciton qubits (but see recent work on adiabatic fast passage with chirped pulses)
- Coherence revivals may be within experimental reach
- Generic system of two level system coupled to boson bath + access to high driving field regime

Summary of Applications of Quantum Dots

1. QD lasers. The main application
2. Mid infra-red detectors
3. Memory devices
4. *Single photon sources, cryptography, entangled photon pairs*

Ensembles (up to 400K)

Single dots (up to ~50K)

Quantum Dots for Telecommunications Lasers

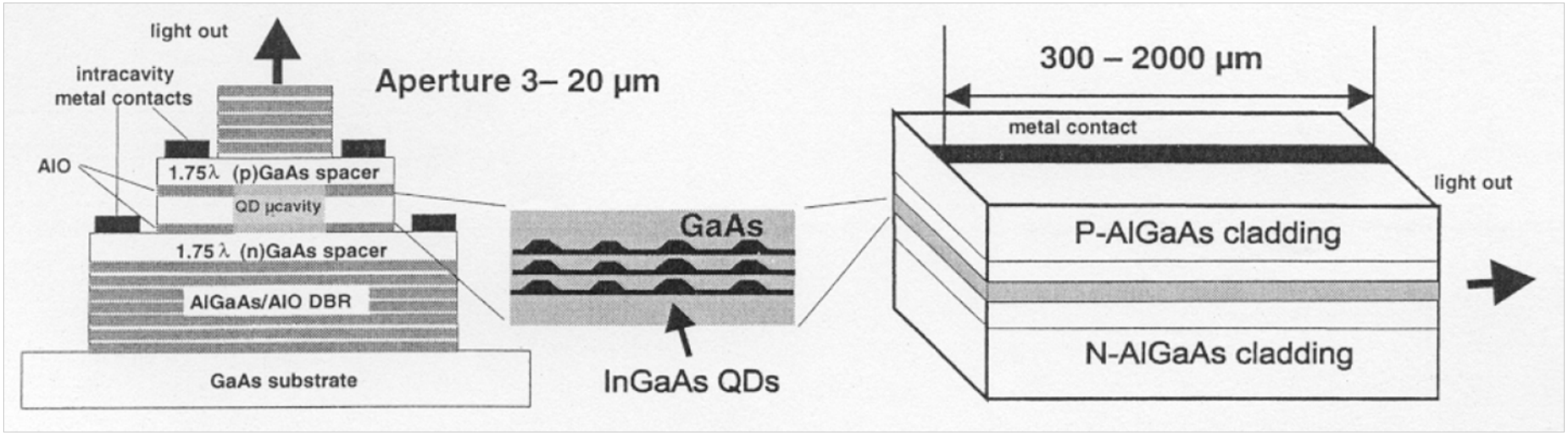

Vertical cavity

Edge emitting

Acknowledgement R A Hogg, for provision of some of slides

Quantum Dot Lasers: Temperature Insensitive

Multidimensional quantum well laser and temperature dependence of its threshold current

Y. Arakawa and H. Sakaki
Institute of Industrial Science, University of Tokyo, Minato-ku, Tokyo 106, Japan

(Received 19 January 1982; accepted for publication 23 March 1982)

A new type of semiconductor laser is studied, in which injected carriers in the active region are quantum mechanically confined in two or three dimensions (2D or 3D). Effects of such confinements on the lasing characteristics are analyzed. Most important, the threshold current of such laser is predicted to be far less temperature sensitive than that of conventional lasers, reflecting the reduced dimensionality of electronic state. In the case of 3D-QW laser, the temperature dependence is virtually eliminated. An experiment on 2D quantum well lasers is performed by placing a conventional laser in a strong magnetic field (30 T) and has demonstrated the predicted increase of T_0 value from 144 to 313 °C.

Predicted that if inter-level energy spacing was >> kT, then QD lasers would be temperature insensitive

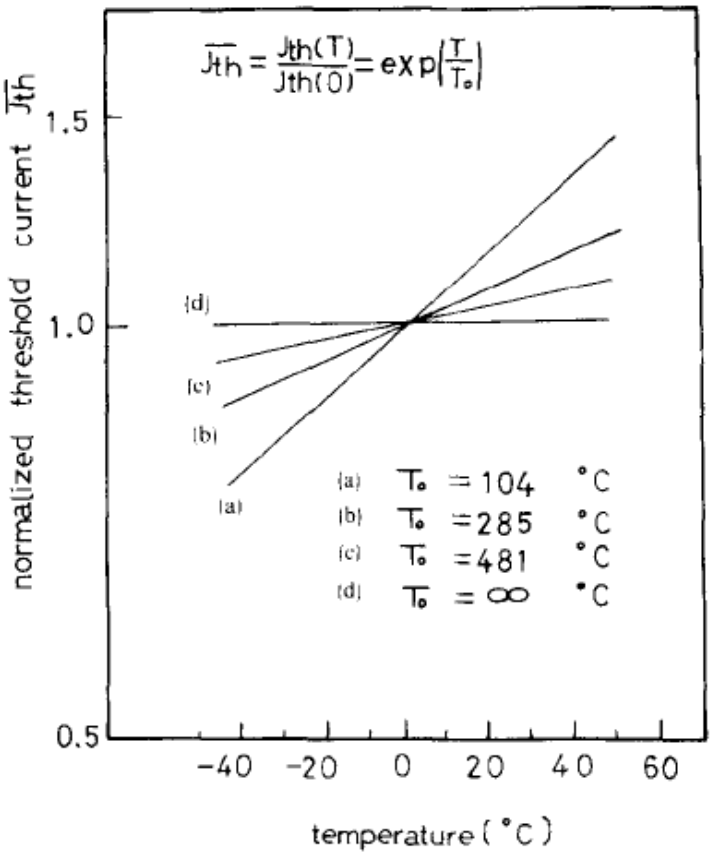

High (Differential) Gain

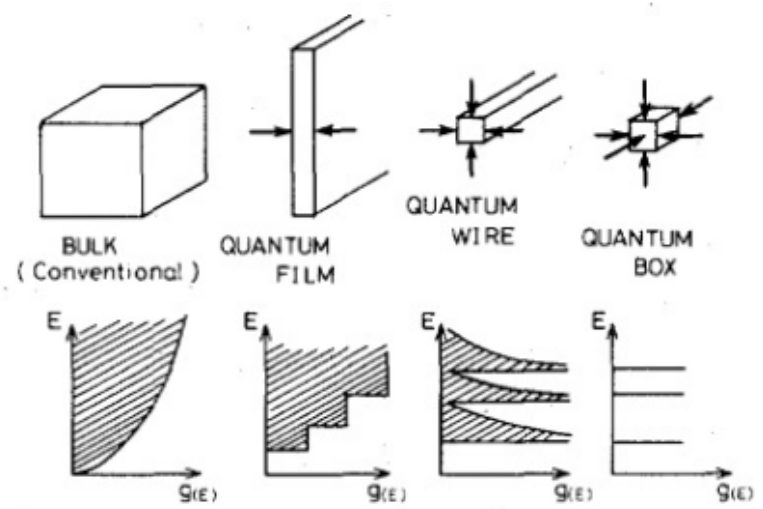

Predicted very high material gain due to 3D confinement

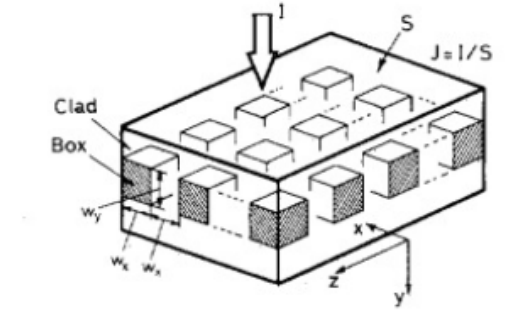

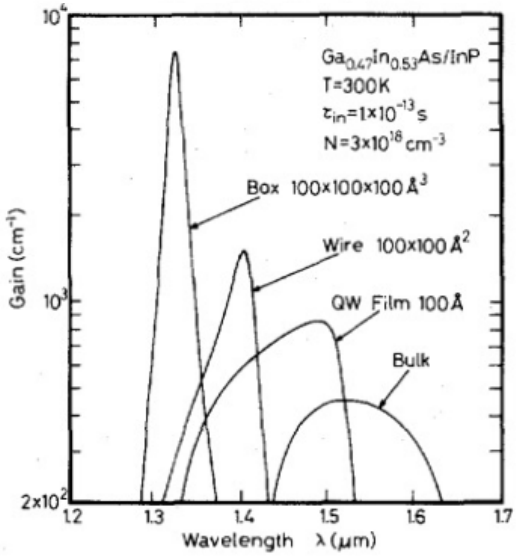

IEEE JOURNAL OF QUANTUM ELECTRONICS, VOL. QE-22, NO. 9, SEPTEMBER 1986 1915

Gain and the Threshold of Three-Dimensional Quantum-Box Lasers

MASAHIRO ASADA, YASUYUKI MIYAMOTO, AND YASUHARU SUEMATSU, FELLOW, IEEE

Quantum Dot Lasers

Breakthrough application, 1.3μm lasers for local area networks

Advantages over installed InP-based lasers (GaAs-based technology, large area substrates, good thermal conductivity, low temperature dependence of threshold current, low cost)

~10 cents per chip
Temperature insensitivity – low module cost as no cooler ~$5 each

High Speed
- ~20 Gbit/second reported
- 10 Gbit/second as product

Semiconductor Laser Performance Versus Year

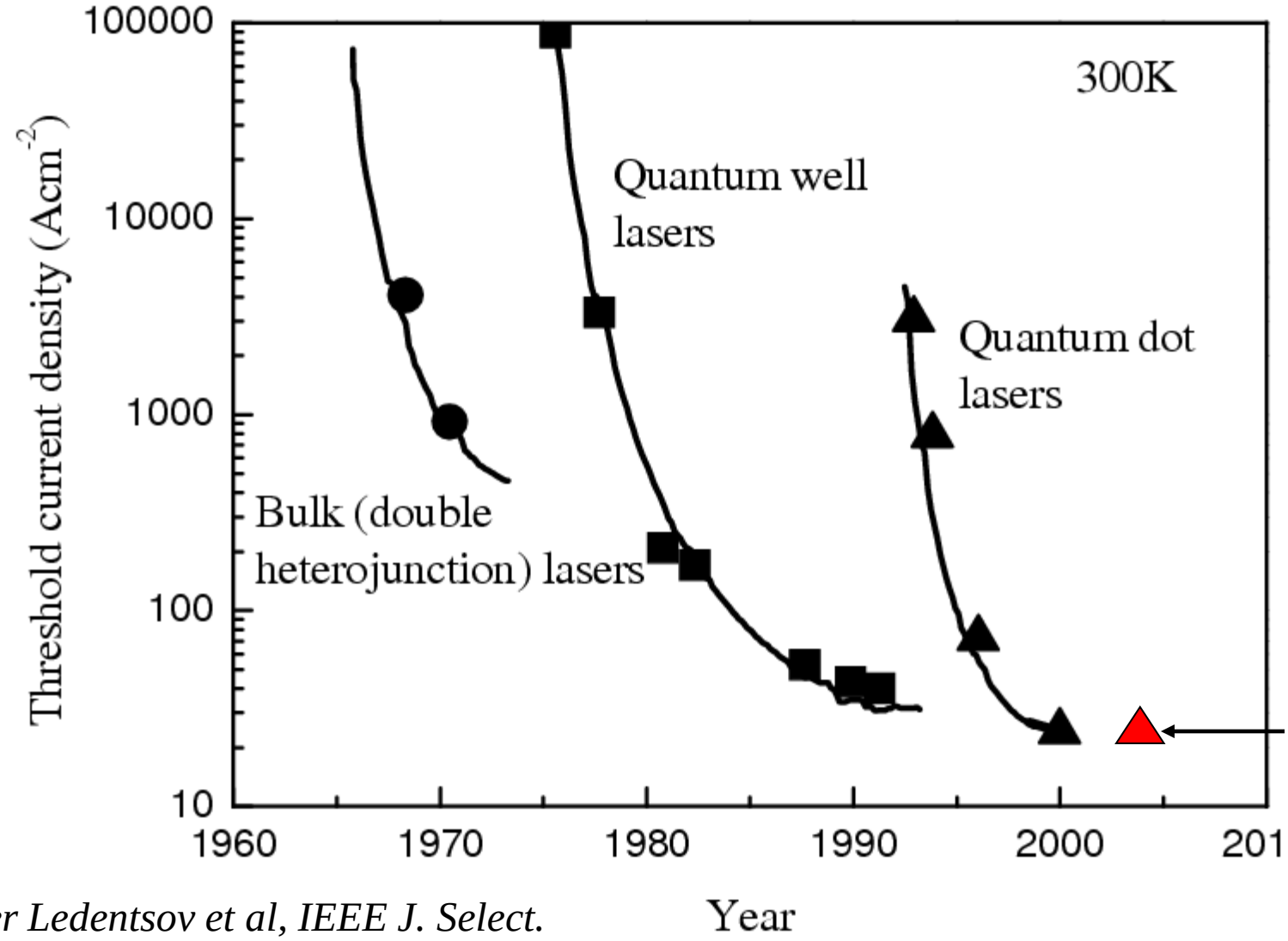

after Ledentsov et al, IEEE J. Select. Topics Quant. Electron. 6, 439 2000

State-of-the-art QD Lasers

- 2 Companies Currently Manufacturing QD Lasers
  - Innolume GmbH (Germany)
  - QD Laser Inc (Japan)

http://www.qdlaser.com/

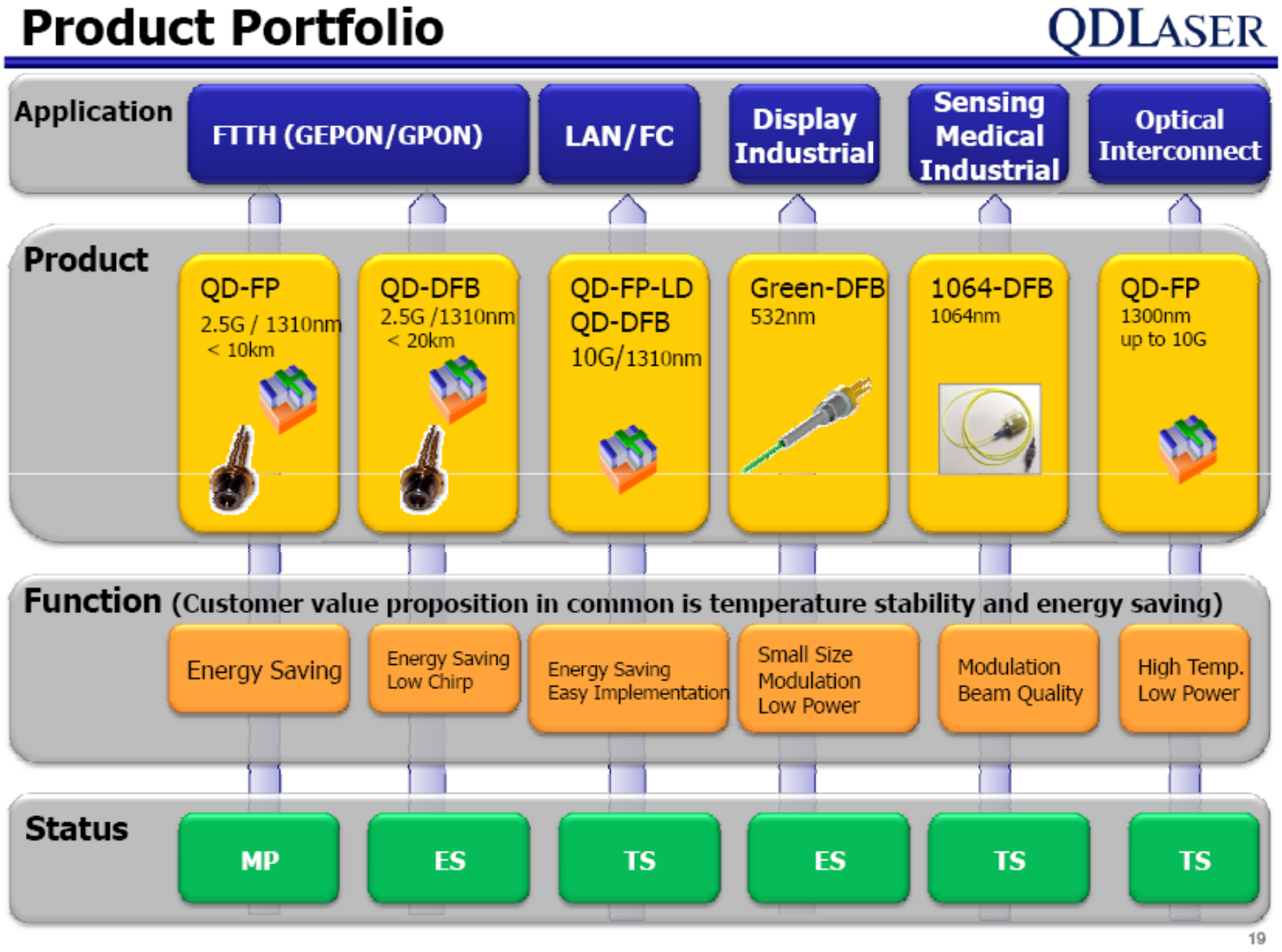

Uncooled High Speed Laser

QD Laser Inc

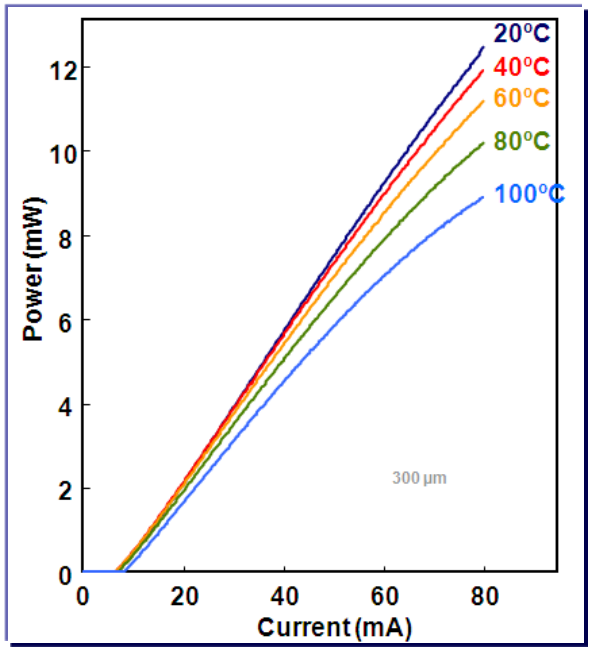

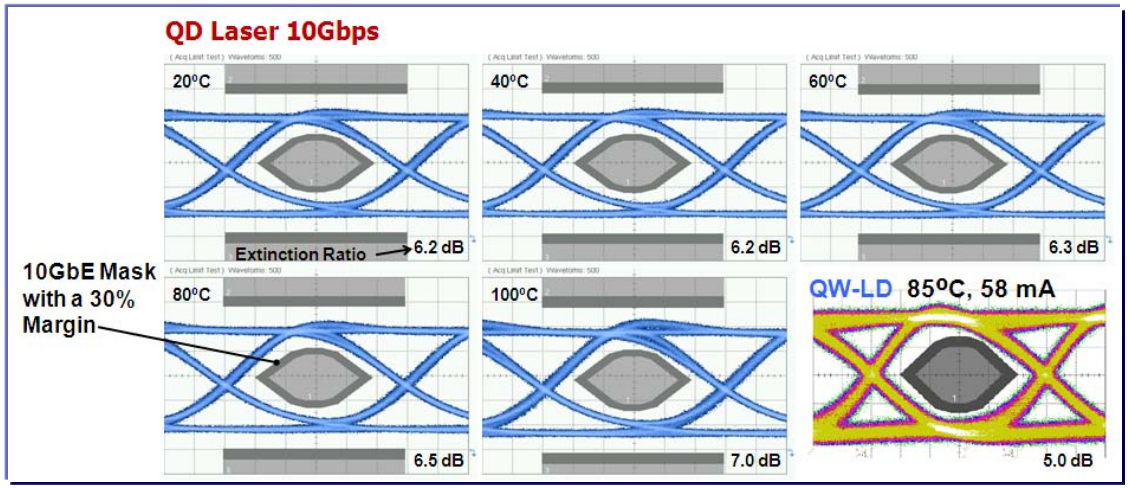

10Gb/s up to 100°C

Very low temperature sensitivity up to 80°C

http://www.qdlaser.com/

Dot in Well Structures (increase wavelength, but retain high density) - engineering of dot properties

1.3μm achieved with high density, good structural properties

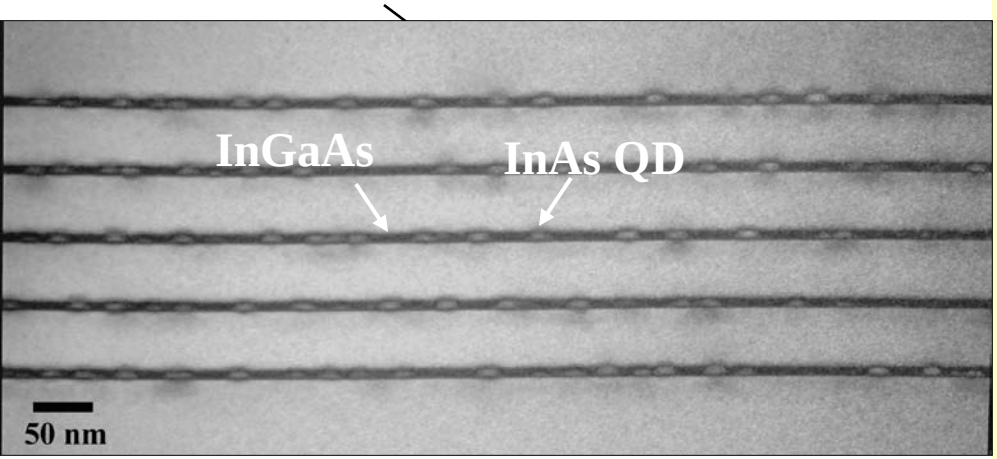

See Liu et al, Appl Phys Lett 85, 704, 2004

DWELL structures

- InAs dots in InGaAs wells
- Increases size of dots
- Reduces strain
- Enables 1.3μm
- High density ~ 3.5 x 10^{10}cm^{-2}
- Commercial now
  6 x 10^{10}cm^{-2}, 8 layers

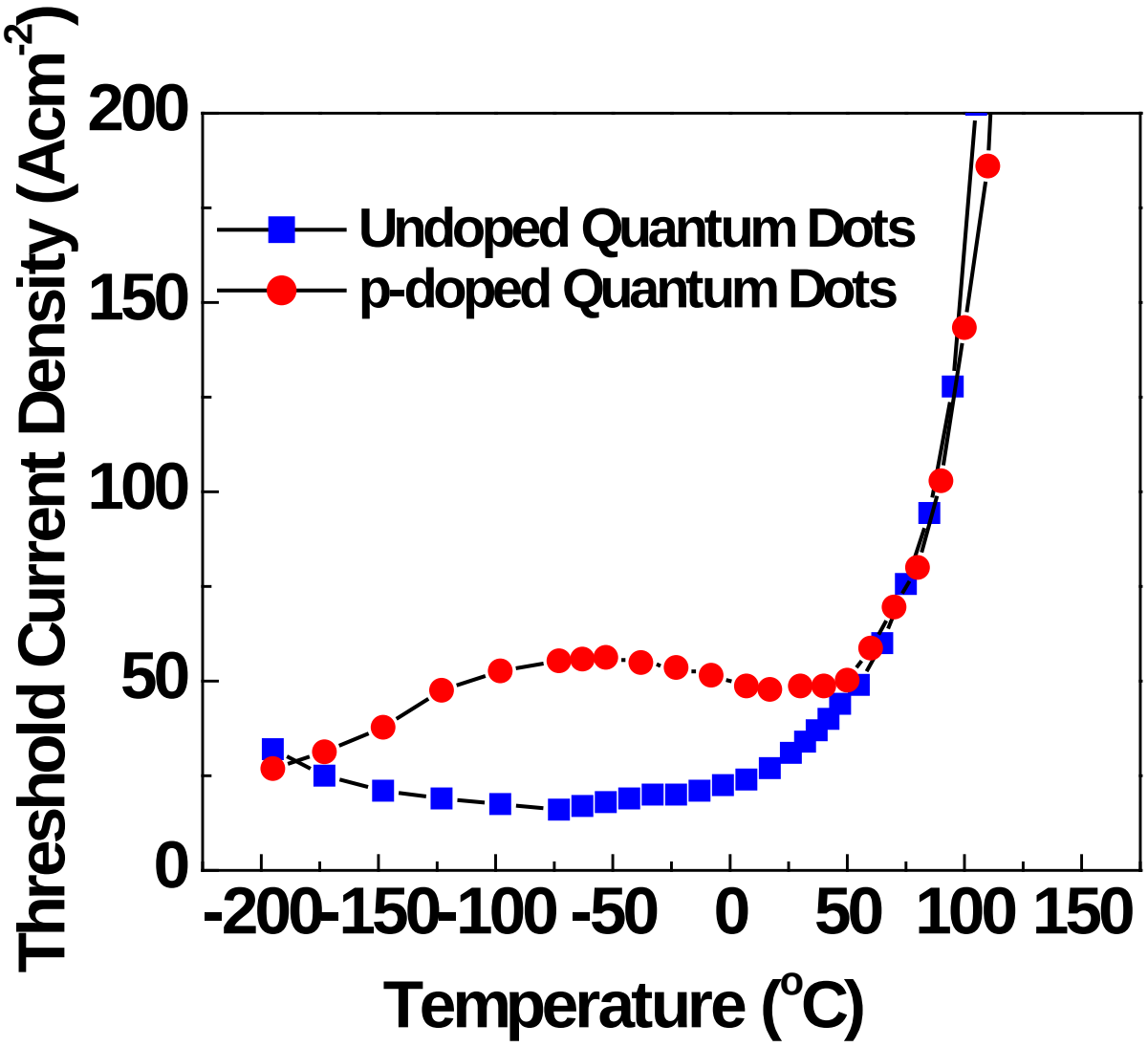

Near temperature independent threshold current density up to 60°C - characteristic of zero D system

Other QD Laser Markets

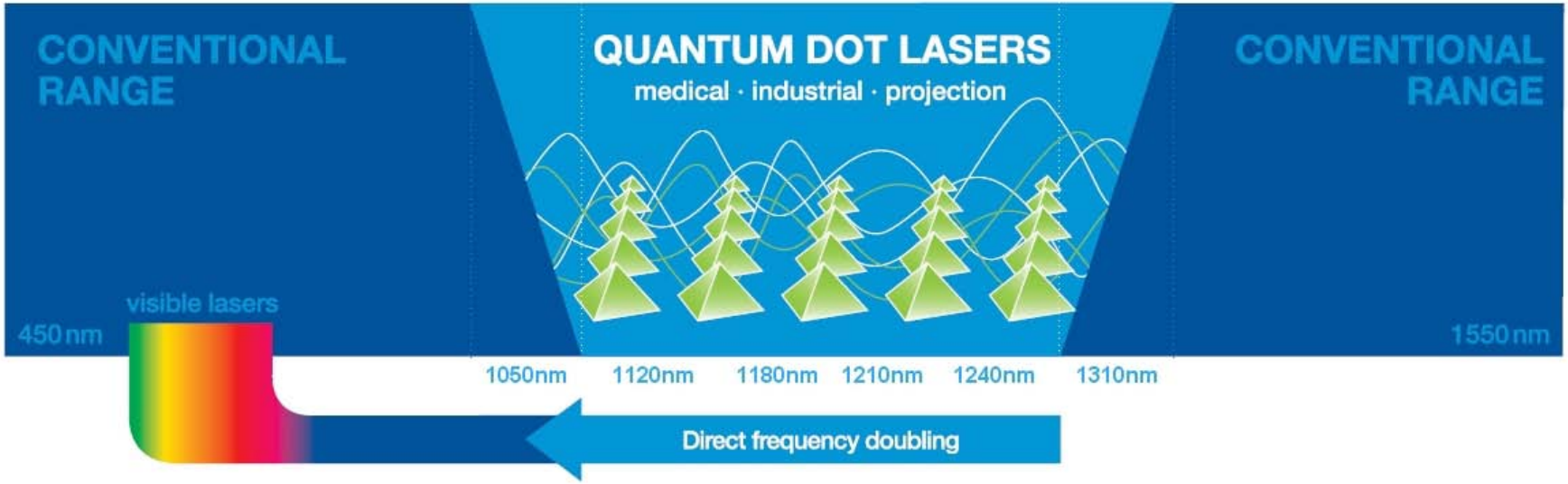

Wide Wavelength Coverage ~1100-1300nm

Second harmonic generation for low power consumption green laser (advantage over GaN based devices due to lower V and I)

Conclusions

1. Quantum dot, atom-like two level systems
2. Fast initialisation, control and readout of carrier spins
3. Exciton-photon coupled states (dressed states)
4. Excitation induced dephasing
5. Coupling of two level system to 3D boson bath
6. Future – integration with cavities, electrical switching, in-situ tuning, coupled dots
7. Applications of quantum dots